Global and Planetary Change xxx (2017) xxx–xxx

Contents lists available at ScienceDirect

Global and Planetary Change

journal homepage: www.elsevier.com/locate/gloplacha

Invited research article

The Amazon at sea: Onset and stages of the Amazon River from a marine record, with special reference to Neogene plant turnover in the drainage basin

Carina Hoorn [a,*], Giovanni R. Bogotá-A [a,b], Millerlandy Romero-Baez [c], Emmy I. Lammertsma [a,d], Suzette G.A. Flantua [a], Elton L. Dantas [d], Rodolfo Dino [e], Dermeval A. do Carmo [d], Farid Chemale Jr [d,1]

[a] Institute for Biodiversity and Ecosystem Dynamics, University of Amsterdam, the Netherlands
[b] Universidad Distrital Francisco José de Caldas, Bogotá, Colombia
[c] Smithsonian Tropical Research Institute, Panama
[d] Institute of Geosciences, Universidade de Brasília, Brasília, DF, Brazil
[e] Petrobras/Cenpes/PDEDS/AMA, Rio de Janeiro, Brazil

ARTICLE INFO

Article history:
Received 19 October 2016
Received in revised form 13 February 2017
Accepted 13 February 2017
Available online xxxx

Keywords:
Miocene
Palynology
Geochemistry
Grasses
Western Atlantic
Amazon submarine fan

ABSTRACT

The Amazon submarine fan is a large sediment apron situated offshore Pará (Brazil) and represents the most distal extent of the Amazon River. The age of onset of this transcontinental river remains debated, yet is of great importance for understanding biotic evolutionary processes on land and at sea. Here we present new geochemical and palynological data from a borehole drilled at the continental slope and dated based on nannofossil biostratigraphy. We found that sediments of mixed source (craton and adjacent) occur at least from the late Oligocene (NP25) to late Miocene (NN9), and that the earliest Andes-derived sediments occur in NN10 (late Miocene). Our geochemical record indicates an onset of the transcontinental Amazon River between 9.4 and 9 Ma, which postdates the regional unconformity by 1 to 1.5 My. The shift in sediment geochemistry is more gradually replicated in the palynological record by a change from coastal plain and tropical lowland taxa to a mixture of tropical lowland, and montane forest to open Andean taxa. In particular, the appearance of taxa such as *Jamesonia* and *Huperzia*, followed by *Valeriana*, *Polylepis-Acaena*, *Lysipomia* and *Plantago* (with a current altitudinal range from 3200 to 4000 m) suggests the development of open, treeless, vegetation between 9.5 and 5.4 Ma, and highlight the presence of a high Andes in the late Miocene hinterland. Poaceae progressively increased from 9 Ma, with a notable rise from 4 Ma onwards, and percentages well above post-glacial and modern values, particularly between 2.6 and 0.8 Ma. We hypothesize that the rise of the grasses is a basin-wide phenomenon, but that the Plio-Pleistocene expansion of open, treeless vegetation on the Andean slopes and foothills are the main contributor. This rise in grasses was likely caused by climatic fluctuations, and subsequent changes in relief and erosion rates. We conclude that the onset of the Amazon River is coupled with Neogene Andean tectonism and that subsequent developments, both of river and biota, are closely linked to the Plio-Pleistocene climatic fluctuations. From latest Neogene onwards these major landscape changes determined the composition of the montane and lowland forest in the Andes-Amazonian system.

1. Introduction

The Amazon River accounts for a fifth of the total volume of fresh water input into the global oceans, it has the highest volume of sediment discharge and also accounts for the largest drainage basin (Nittrouer and DeMaster, 1986; Milliman, 2001). In spite of its global importance, the age of onset of the transcontinental Amazon River is still subject of debate. It divides scientists depending on the type of data set (marine- or land-derived) and the analytical methods that are applied (e.g. seismic stratigraphy, geochemistry, sedimentology, phylogeography).

Marine data from the westernmost Atlantic point to a late Miocene age of onset of the Amazon River (Damuth and Kumar, 1975; Milliman, 1979; Hoorn et al., 1995; Dobson et al., 2001; Pasley et al., 2005; Figueiredo et al., 2009, 2010; Gorini et al., 2013). Instead, continental data are taken as indicative for a Plio-Pleistocene age of onset

* Corresponding author.
E-mail address: M.C.Hoorn@uva.nl (C. Hoorn).
[1] Present address: Universidade do Vale do Rio dos Sinos, São Leopoldo, Brazil.

http://dx.doi.org/10.1016/j.gloplacha.2017.02.005
0921-8181/

(Rossetti et al., 2005, 2015; Campbell et al., 2006; Campbell, 2010; Latrubesse et al., 2010; Ribas et al., 2012; Horbe et al., 2013). Considering the global and regional influence of the Amazon River on continental and marine processes (Davidson and Artaxo, 2004; Subramaniam et al., 2008; Yoon and Zeng, 2010) the age of its onset is thus a matter of the highest interest for the wider scientific community including biologists, geoscientists and paleoceanographers.

To resolve this debate it is important to define the key characteristics of the Amazon River and use these parameters in the research set up. According to the Encyclopedia Britannica (2016) the Amazon has "*its westernmost source high in the Andes Mountains, within 100 miles (160 km) of the Pacific Ocean, and its mouth is in the Atlantic Ocean, on the northeastern coast of Brazil*". This implies that an inherent characteristic of the Amazon River is it's birth in the Andes and it's end in the Atlantic. Extending on the geographical definition, sedimentologists and geochemists describe the characteristic mixed sediment load of the modern Amazon River as of predominantly Andean origin with a significant tropical lowland component (Gibbs, 1967; Meade, 1994; McClain and Naiman, 2008). Taken together, this means that the oldest Amazon River sediments should: a) be found in the westernmost Atlantic and, b) have an Andean geochemical signature. This makes the Amazon submarine fan, a sediment apron formed by Amazon River deposits along the Atlantic Coast (Damuth and Kumar, 1975), the perfect setting to study the evolution of this river.

The Amazon submarine fan deposits were accumulated in the Foz do Amazonas Basin (FAB), a sedimentary basin situated at the Brazilian Equatorial Margin (BEM), where the Cretaceous-Cenozoic sedimentary succession is relatively complete (Fig. 1A and B) (Figueiredo et al., 2007). In this respect, the oceanic record strongly contrasts with the continental basins in Amazonia, where a more fragmented stratigraphy is preserved. Academic drilling programs, such as the Ocean Drilling Program (ODP), have focused on the uppermost Pleistocene section in the distal submarine fan. Yet the pre-Quaternary sedimentary section so far remained out of reach (Flood et al., 1995). Nevertheless, the FAB has been well studied by the industry because of its presumed hydrocarbon potential. Most of this extensive knowledge and data archive is confidential though. Exceptions are published work on evolutionary stages of the Amazon submarine fan (Pasley et al., 2005; Figueiredo et al., 2007, 2009; Gorini et al., 2013).

The recent (partial) disclosure of borehole data of an exploration well, known as Algodoal or BP3, by the Brazilian oil company Petrobras and the Agência Nacional do Petróleo, Gás Natural e Biocombustíveis (ANP), presents an exceptional opportunity to investigate the age and evolution of the transcontinental Amazon River. This well (here Well 2) was previously described by Figueiredo et al. (2009) and is situated on the upper slope of the continental shelf at a water depth of 754 m (Fig. 1B). In this section an almost complete Neogene stratigraphy occurs with ages well constraint by nannofossil biostratigraphy (Varol Research, 2004; Figueiredo et al., 2009).

In this study we review the general stratigraphy of the FAB, and combine the results of our geochemical and palynological study from the Neogene section of Well 2 into a new model for the evolution of the Amazon River. In this model we link changes in sediment and pollen source area to an expanding drainage basin, that shifts from a proto-Amazon River in eastern Amazonia to the continent-wide transcontinental Amazon drainage basin as we know it today. We also observe that changes in biotic composition likely occurred in parallel with the Neogene landscape changes.

2. Regional geological framework

On arrival at the western tropical Atlantic Ocean the Amazon River sediments are partially deposited in the subaqueous delta (Nittrouer and DeMaster, 1986; Nittrouer et al., 1986; Nittrouer and DeMaster, 1996), in Portuguese this is called the Foz do Amazonas or 'mouth of the Amazon', and it is also the name of the sedimentary basin that records the marine extent of the Amazon River in the Atlantic Ocean (Fig. 1B). The bulk of the Amazon River sediments, however, are transported towards the Caribbean by the North Brazil Current (Nittrouer and DeMaster, 1996, and references therein). From May to October, a retroflection of this current also moves a fraction of the sediments towards Africa via the North Equatorial Counter Current

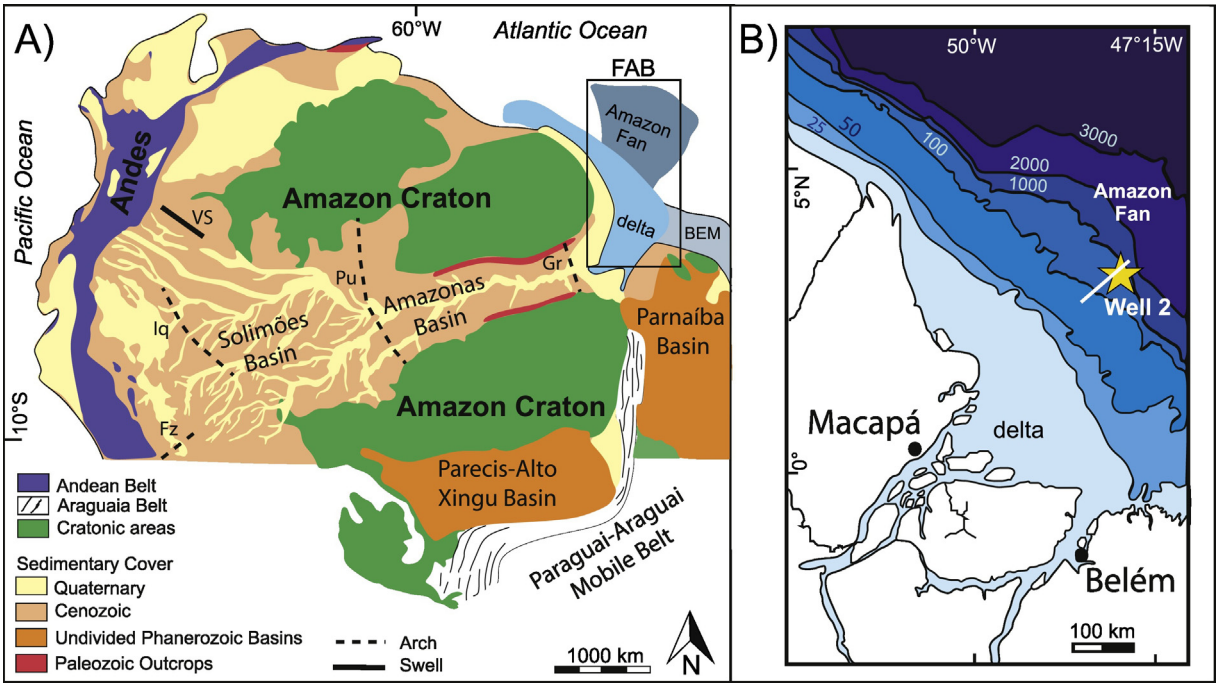

Fig. 1. A) Overview map of northern South America with the location of the Amazon drainage basin, and the geological units that formed the provenance area for the sediment input into the Amazon River through it different stages. The Amazon subaqueous delta and submarine fan are in the inset. The following structures are abbreviated, Archs: Fitzcarrald (Fz), Iquitos (Iq), Purus (Pu) and Gurupá (Gr); and Swell: Vaupes (VS). 1B) The location of Well 2 and the seismic section in the Foz do Amazonas Basin; the contours of water depth are indicated in meters.

Please cite this article as: Hoorn, C., et al., The Amazon at sea: Onset and stages of the Amazon River from a marine record, with special reference to Neogene plant turnover in ..., Glob. Planet. Change (2017), http://dx.doi.org/10.1016/j.gloplacha.2017.02.005

(Muller-Karger et al., 1988; Wilson et al., 2011). This configuration also existed in the past during phases of sea level highstand (see e.g. Heinrich and Zonneveld, 2013). Instead, during sea level lowstand, such as in the glacial Pleistocene, the bulk of the sedimentary load of the Amazon River was deposited in the FAB (Figueiredo et al., 2009).

The FAB is situated on the BEM, a passive continental margin that extends from easternmost Brazil to the border with French Guyana, and was formed during the Mesozoic rift event that opened up the Atlantic Ocean (Brandão and Feijó, 1994). This basin holds sediments of around 10 km in thickness, a load that has caused the relatively thin oceanic crust to buckle under its weight while deforming the coastal topography (Driscoll and Karner, 1994; Watts et al., 2009). The overall architecture of this sedimentary basin and the stratigraphic sequence boundaries are well documented (Milliman, 1979; Pasley et al., 2005; Figueiredo et al., 2007; Gorini et al., 2013) and the sedimentary record of the Amazon submarine fan, as observed on the shelf and continental slope, is described by Figueiredo et al. (2009, 2010).

The post-rift succession in the FAB is formed by the clastic Limoeiro Formation, which extends from the Cretaceous into the lower Paleocene. Carbonate deposition initiates at the shelf from around 60 Ma (Amapá Formation). At the high end of the shelf these carbonates interfinger with coarse clastic sediments (Marajó Formation), and at the continental slope they interfinger with fine clastic sediments (Travosas Formation). During sea level highstand fine, clastic sedimentation occurs on the shelf, whereas during sea level lowstand coarse clastic sedimentation extends towards the ocean, onto the slope and towards deeper waters (e.g. Pasley et al., 2005).

During the Paleogene and the early Neogene, clastic sediment input was relatively low and had its provenance in the Amazon Craton and Paraguai-Araguai Mobile Belt and Phanerozoic basins (Fig. 1A). This resulted in a mixed carbonate and siliciclastic sequence (Milliman, 1979; Figueiredo et al., 2009; Gorini et al., 2013), which was truncated by a late Miocene regional unconformity that coincided with a global sea level lowstand (Pasley et al., 2005; Figueiredo et al., 2009; Gorini et al., 2013). The arrival of large volumes of clastic sediments in the FAB during the late Miocene smothered the carbonate factories and brought carbonate deposition almost to a halt (Figueiredo et al., 2009; but see Moura et al., 2016). On the shelf these sediments are known as Tucunaré Formation, and on the slope and in the deep sea these siltstone and mudstones are respectively called Pirarucu and Orange Formation.

The late Miocene unconformity was also observed in the Suriname-Guyana Basin (situated northwestwards of the FAB) and, like in the FAB, Andes-derived sediments here too ended carbonate production (Campbell, 2005). Meanwhile, in the Pará-Maranhão Basin situated southeastwards of the FAB, carbonate production continued undisturbed (Soares et al., 2007). In this basin deposition of a mixed succession of clastic sediments and carbonate continues until present. During the latest Miocene sedimentation rates increased in the submarine fan, and multiplied further during the Pleistocene (Figueiredo et al., 2009). The latest Pleistocene-Holocene sequence, situated at the distal extent of the submarine fan, is extensively documented by ODP leg 155 (Flood et al., 1995; Flood and Piper, 1997).

3. Well site and lithostratigraphy

Throughout the '70s and '80s Petrobras led an extensive exploration campaign in the FAB, and a more recent campaign at the beginning of the 21st century. Well 2 was part of this latest effort and was drilled as exploration well by a consortium formed by BP, Shell and Total. Data were confidential until 2015, but are now partially released by ANP. This well is situated at latitude 3° 2′ 58,660″N and longitude 47° 44′ 45,801″ W (Fig. 1B) and was drilled in 754 m water depth. Ditch cutting samples, the only sample type available for this region, were made available to us by Petrobras. The age determination for Well 2 is based on nannofossil biostratigraphy (Varol Research, 2004; Figueiredo et al., 2009, 2010) and selected information is cited with permission from ANP.

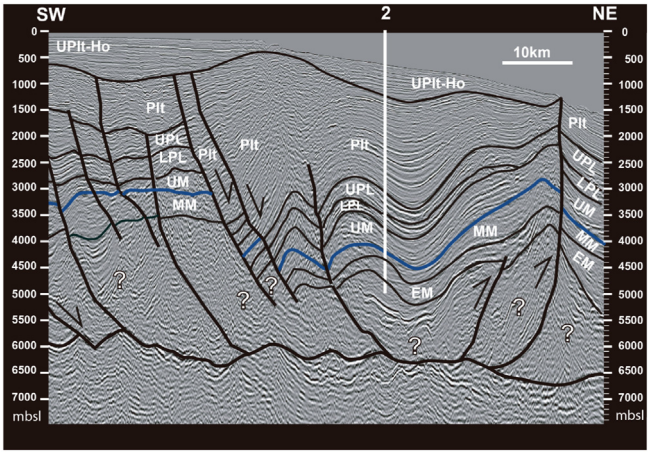

Fig. 2. Simplified interpretation of the seismic stratigraphy in the Foz do Amazonas Basin in the area of Well 2. The location of Well 2 is extrapolated on this seismic line. The stratigraphic section is subdivided into upper Miocene (UM), lower Pliocene (LPL), upper Pliocene (UPL) and Pleistocene (Plt). The contact between the pre-Fan (MM = Middle Miocene) and Fan (UM = Upper Miocene) is shown in blue. Depth is in meters below sea level (mbsl).

In Fig. 2 we show a seismic interpretation of the studied section with the extrapolated position of Well 2. In this region the Neogene section is strongly controlled by SW-orientated extensional- and NE-orientated compressional faulting, which is attributed to the tectonic arrangement of the submarine fan due to the thick sedimentary overloading and probable deformation at the margin of South America Plate. Cobbold et al. (2004) relate these structures to thin-skin tectonics and slope instability. This tectonism led to folding and faulting of the Amazon Fan sedimentary package, but did not affect the upper Pleistocene to Holocene section.

In this study we analyzed the sedimentary succession comprised between 4734 and 1502 meters below sea level (mbsl), with geochemical analysis restricted between 4633 and 2616 mbsl. This section was dated as latest Oligocene (NP25) to Pleistocene (NN19) (Fig. 3; Appendix A). The Travosas Formation forms the base of the section and occurs up to 4178 mbsl. From that level and up to the top of the section (at 754 mbsl) is formed by the Orange Formation. Five casings were placed over the sampled section during drilling to prevent caving of the well (Appendix A).

A mixed succession of siltstones and mudstones of 20 to 80 m thickness, and carbonates of up to 5 m occurs between 4734 and 4139 mbsl. The last carbonate deposit is found at about 4100 mbsl, and from there until the top of the section (at 1502 mbsl) only clastic sediments occur (Varol Research, 2004). However, up to 3624 mbsl the mudstone and siltstone often carry calcareous fragments, possibly reworked from the continental shelf.

A major stratigraphic break is reported between 4145 and 4139 mbsl (NN7 to NN9 respectively), and the top of the unconformity is marked by the first occurrence of *Discoaster hamatus* (Figueiredo et al., 2009) (Fig. 3; Appendix A). Other stratigraphic breaks occur at 3328 mbsl (NN15–16; lower - upper Pliocene) and at 2644 mbsl (NN18-NN19; upper Pliocene - lower Pleistocene) (Varol Research, 2004; Figueiredo et al., 2009).

4. Provenance from geochemistry and palynology

4.1. Geochemistry

River sediments carry a unique geochemical fingerprint that can link them to their source area. Allègre et al. (1996) showed that the suspended matter in the main course of Amazon River and its tributaries

Please cite this article as: Hoorn, C., et al., The Amazon at sea: Onset and stages of the Amazon River from a marine record, with special reference to Neogene plant turnover in ..., Glob. Planet. Change (2017), http://dx.doi.org/10.1016/j.gloplacha.2017.02.005

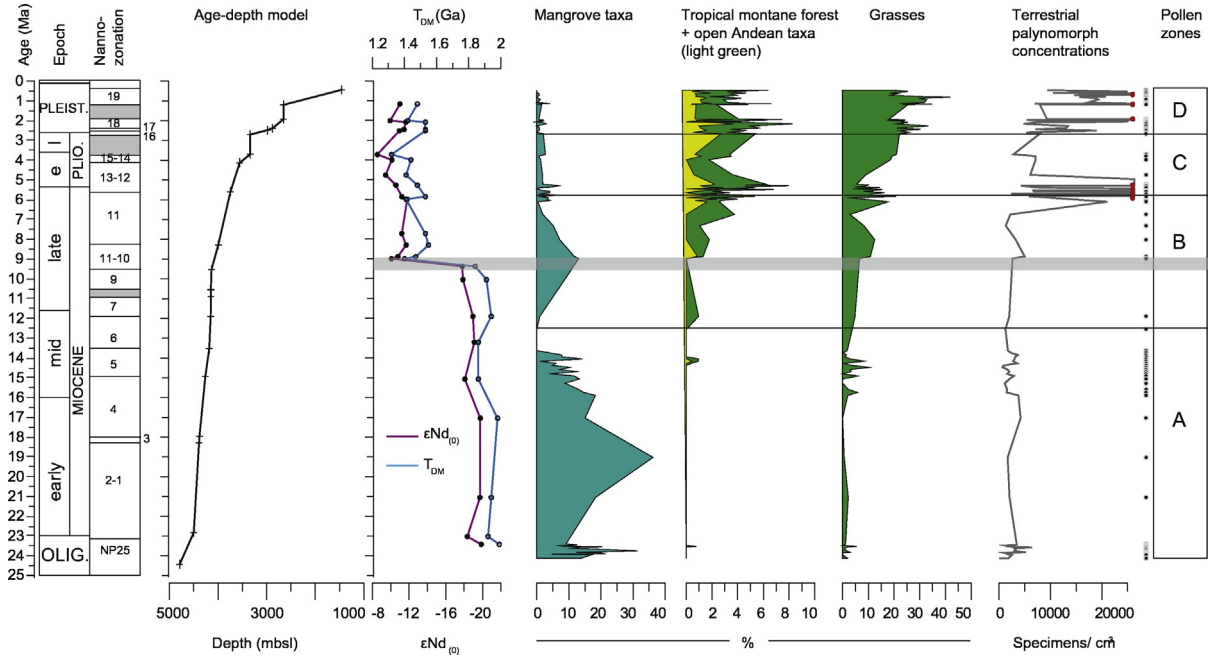

Fig. 3. Overview diagram with the most important information from Well 2 in relation to the new data from this study. Plotted to age we show the nannozonation (grey bars indicate hiatuses, see Appendix A); age-depth model (+indicate zone boundaries dated to Gradstein et al., 2012), the εNd(0) and T_{DM} (sampled depths indicated by closed and open circles, respectively); relative abundances of most relevant plant groups - mangrove taxa, tropical montane forest and open Andean taxa (stacked), and grasses; terrestrial palynomorph concentrations (red dots indicate outliers). Palynological sample depths are indicated by grey/black dots. The pollen zonation is explained in the text, and further details can be found in the complete palynological diagram in Fig. 5. The grey horizontal bar indicates the transition from pre-Fan to Fan (9.4–9 Ma).

carry a geochemical signature that is derived from the geological units within the river's drainage basin.

In this work, we use samarium (Sm) - neodymium (Nd) isotope data to determine the geochemical fingerprint of the sediment source in the Amazon Fan (Fig. 4A). Nd and Sm isotopes provide very important information on rare elements of the reservoir of which the rocks are derived (DePaolo, 1988). The epsilon (ε) Nd values and Nd model age (Nd T_{DM} age) are used to characterize geological material (protholiths) derived from the mantle or derived from crustal reworked source or even mixed sources in different proportions. In addition to that, a combination of model age of whole rock (WR) is also used to estimate the mean crustal residence of continental crust (clastic sediments or their metamorphic rocks as schists and gneisses) (DePaolo, 1981). The $\varepsilon Nd_{(present\text{-}day\ or\ 0)}$ and Nd model age (T_{DM}) are defined by:

$$\varepsilon Nd_{(0)} = \left[\frac{\left(^{143}Nd/^{144}Nd\right)_s^0}{\left(^{143}Nd/^{144}Nd\right)_{chur}^0} - 1\right] \times 10^4$$

where $^{143}Nd/^{144}Nd_{chur(today)} = 0.512638$ and $^{143}Nd/^{144}Nd_{s\ (sample,\ now)}$ is the measured ratio of analyzed sample.

$$T_{DM} = \frac{1}{\lambda}\ \ln\left(\frac{\left(^{143}Nd/^{144}Nd\right)_0 - \left(^{143}Nd/^{144}Nd\right)_{DM}}{\left(^{147}Sm/^{144}Nd\right)_0 - \left(^{147}Sm/^{144}Nd\right)_{DM}} + 1\right)$$

where the measured isotope values (sample, now) are $^{143}Nd/^{144}Nd_0$ and $^{147}Sm/^{144}Nd_0$; and DM ratios are those Sm-Nd isotope ratios calculated for depleted mantle (DM).

Both values can be used to trace the contribution of older crustal material (the Amazon Craton rocks or reworked Phaneorozoic sedimentary rocks) versus that of younger material (Andean material). This implies that rivers born on basement rocks, such as the Amazon Craton, present negative values of εNd ranging from −17 to −45 (present-day = 0) and Nd model age of 1.75 Ga to 3.3 Ga (Cordani and Sato, 1999). The Nd isotope signature of suspended matter from river tributaries which drain basement rocks and reworked Phanerozoic rocks should thus have mean εNd values equal or lower than −17 and an older Nd model age (T_{DM}) than 1.75 Ga. On the other hand, the Andes mountains are mainly made up of Phaneorozic rocks and the expected model age and $\varepsilon Nd_{(0)}$ would be in the same range as that found by Basu et al. (1990) for fluvial sediments of the Madre de Dios river, which range from −8.02 to −11.55 (see ellipse of Fig. 4B) and T_{DM} lower than 1.6 Ga.

Nd isotopes studies carried out in the Amazon Fan sediments and sedimentary rocks presented by McDaniel et al. (1997) and Figueiredo et al. (2009), respectively, showed that most of sediments deposited in the Amazon Fan contain a fingerprint of Andean signature. The values obtained by Basu et al. (1990) properly reflect an admixture of juvenile Andean material in different proportions with older material and those form most of the volume of rocks in the lithosphere. The aforementioned studies allow us to differentiate between the cratonic and the Andean signal through their $\varepsilon Nd_{(0)}$ values (Figs. 3 and 4A) and/or T_{DM}.

4.2. Palynology

The submarine fan environment is a good trap for terrestrial organic matter, including sporomorphs, which accumulates within the complex of submarine channels and distributaries. Once at the ocean the terrestrial component is further admixed with marine palynomorph components such as organic-walled dinoflagellate cysts and foraminiferal linings (Hoorn, 1997; Beaudouin et al., 2004). Depending on the proportion of the terrestrial input, the sediments recovered from such marine environment can closely resemble those of a terrestrial fluvial system.

The Quaternary sediments in the distal Amazon submarine fan are well documented and contain palynomorphs of a wide variety of terrestrial sources (Haberle, 1997; Hoorn, 1997; Haberle and Maslin, 1999). These are sorted depending on seasonality, the proximal or distal position to the coast, depositional environment and position within the turbidite sequence (e.g. Heusser, 1988; Haberle, 1997; Hoorn, 1997; Beaudouin et al., 2004; Mildenhall and Orpin, 2010). The palynological

Please cite this article as: Hoorn, C., et al., The Amazon at sea: Onset and stages of the Amazon River from a marine record, with special reference to Neogene plant turnover in ..., Glob. Planet. Change (2017), http://dx.doi.org/10.1016/j.gloplacha.2017.02.005

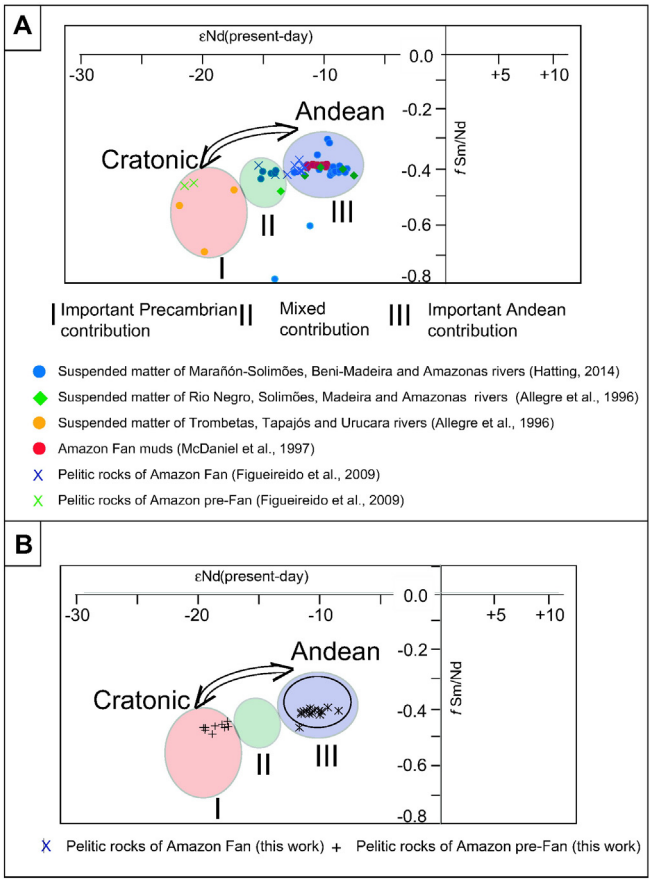

Fig. 4. Summary diagram of the sediment geochemistry in Well 2. A. Epsilon Nd (present-day) versus *f* Sm/Nd diagram for suspended matter in the Amazon River and its tributaries, and muds and pelitic rocks from the Amazon subaqueous delta and submarine fan (modified after Allègre et al., 1996; McDaniel et al., 1997; Figueiredo et al., 2009; Hatting, 2014). Two samples outside the fields (I, II, and III) have a significant Sm-Nd isotope fractionation. Field I is defined by an important admixture of clay and silt from the Precambrian rocks or recycled Phanerozoic (mainly Paleozoic) in suspended matter of the Amazonian-born rivers and pelitic sediments in the Amazon subaqueous delta and submarine fan. Field II represents a mixed signal of Andean and Precambrian source, suggesting a balanced sediment contribution from both sources. An important admixture of clay and silt of Andean provenance defines Field III. B. The same diagram with the fields defined by their provenance after Nd isotope data with the pelitic sediments that were analyzed in this work. The black circle in the Field III represents the distribution of the fluvial sands collected at headwaters of Amazon River in the Andean foreland, which contains an important signal or signature of rocks derived from the Andes (see explanation in the text).

data set gives us both an impression of the overall composition of the terrestrial biomes and on the paleoelevation types in the drainage basin.

5. Material and methods

5.1. Age-depth model

The nannofossil biostratigraphy by Varol Research (2004) follows Martini (1971) (but see Appendix A) and all biostratigraphically relevant taxa are listed in Appendix A. The ages of the nannofossil zone transitions follow Gradstein et al. (2012) and are used as tie-points in the age-depth model (Fig. 3). Linear sedimentation rates are assumed between the tie-points, as more detailed information is not available. The durations of the three stratigraphic breaks are estimated based on missing nannofossil (sub)zones and thus represent a minimum duration. Smaller hiatuses may be present but go unnoticed between the tie-points. Based on this age-depth model ages for sampled depths are calculated using software AnalySeries 2.0 (Paillard et al., 1996).

Besides the nannofossil biostratigraphy, we also document the most common Neogene palynostratigraphic markers (following Jaramillo et al., 2011) that were found in the studied section of northern South America and we relate these to the nannostratigraphic zonation scheme.

5.2. Geochemistry

We analyzed the Sm and Nd isotope ratio of 24 selected ditch cutting samples from Well 2 (Table 1), 9 from the pre-Fan section and 15 samples from the Fan section. Whole-rock powders (~100 mg of sample powder) were spiked with a combined ^{150}Nd-^{149}Sm tracer and dissolved using a solution of 5:1 HF-HNO_3 in Savillex® vials on a hot plate. After cooling and evaporation of the HF-HNO_3 solution, samples were re-dissolved in the Savillex® vials with 7 ml of 6 N HCl, evaporated, and then taken up in 3 ml of 2.5 N HCl. The chemical extraction of Sm and Nd follows the conventional chromatographic procedure described by Gioia and Pimentel (2000) using LN-Spec resin in Teflon columns. Column procedures used cationic AG-50W-X8 (200–400 mesh) resin and Rare Earth Elements (REE), followed by Sm and Nd separation using anionic HDEHP LN-B50-A (100-200 μm) resin according to procedures described by Gioia and Pimentel (2000). Each sample was dried to a solid and then loaded with 0.25 N H_3PO_4 on appropriated filament (Ta for Sm and Re for Nd). All samples were analyzed using a Thermo Scientific TRITON™ Plus Thermal Ionization Mass Spectrometer (TIMS) operating in the static multi-collector mode at the Laboratory of Geochronology of University of Brasília.

We typically collected 100–120 ratios with a 0.5 to 1-V ^{144}Nd beam. Nd ratios were normalized to $^{146}Nd/^{144}Nd = 0.7219$. All analyses were adjusted for variations in instrumental bias due to periodic adjustment of collector positions as monitored by measurements of laboratory internal standards. Repeated measurements on the USGS BHVO-1 standard gave $^{143}Nd/^{144}Nd = 0.512996 \pm 0.000006$ (2SD; $n = 7$) during the course of this study. Nd isotope analyses were normalized to a common value of 0.512957 for BHVO-1 (Raczek et al., 2003). Average blank values were <150 pg/g for Sm and <300 pg/g for Nd. Correction for blank was insignificant for Nd isotopic compositions and generally insignificant for Sm/Nd ratios. Neodymium crustal residence (or depleted mantle) model ages (T_{DM}) were calculated following the depleted mantle model of DePaolo (1981). We also applied a *t*-test analysis on the results of the sample analysis from the pre-Fan and Fan section and statistically compare the two groups.

5.3. Palynology

5.3.1. Processing method

A total of 123 ditch cutting samples were processed for pollen analysis. For each sample a volume of about 1.5 cm^3 was decalcified with hydrochloric acid, followed by sodium pyrophosphate, acetolysis and bromoform separation of the inorganic fraction; the resulting organic residues were kept in glycerine solution. A tablet with *Lycopodium clavatum* spores was added at the beginning of the process in order to estimate the pollen concentration in the sediment.

Pollen analysis was performed at ×400 magnification. From the 123 samples, 98 samples reached a pollen sum of >50 grains, but when possible 200 well-preserved sporomorphs (pollen grains and fern spores) were counted per sample as basis for a percentage diagram. The pollen sum is chosen to reflect changes in terrestrial vegetation cover of the Amazonian lowlands and the Andes mountains, and therefore includes all pollen and fern spores. Foraminifer linings, organic-walled dinoflagellate cysts (dinocysts), corroded, folded or reworked sporomorphs are excluded from the pollen sum and represented proportional to the pollen sum. The sporomorphs were tentatively grouped according to the ecological preferences of the nearest living relatives in the Amazon drainage basin (Appendix B). The sample depth and corresponding ages are listed in Data Repository 1, and the percentages of the

Table 1
Sm-Nd isotope data for samples of pelitic rocks from well 2.

Sample #	Depth (mbsl)	Sm (ppm)	Nd (ppm)	$^{147}Sm/^{144}Nd$	$^{143}Nd/^{144}Nd$	±2SE	*f*sm/Nd	eNd (0)[a]	TDM[b] (Ga)	Stratigraphic age[c]
1	2591	6.4	33.8	0.115	0.512074	11	−0.42	−11.0	1.48	1.2
2	2690	7.1	37.1	0.116	0.512128	14	−0.41	−9.9	1.42	2.0
3	2726	6.6	34.5	0.115	0.512041	3	−0.42	−11.7	1.53	2.1
4	2942	7.3	38.0	0.116	0.512052	16	−0.41	−11.4	1.53	2.4
5	3023	7.0	35.8	0.119	0.512077	17	−0.40	−10.9	1.53	2.5
6	3347	6.6	34.3	0.117	0.512200	16	−0.41	−8.6	1.32	3.7
7	3482	7.2	37.2	0.117	0.512118	18	−0.41	−10.1	1.44	4.0
8	3635	5.7	28.8	0.119	0.512154	26	−0.40	−9.4	1.41	4.8
9	3702	6.3	32.3	0.117	0.512096	10	−0.40	−10.6	1.48	5.3
10	3768	7.5	38.8	0.117	0.512063	11	−0.41	−11.2	1.53	5.8
11	3780	4.8	27.6	0.105	0.512033	11	−0.46	−11.8	1.41	6.0
12	3942	6.1	31.4	0.117	0.512064	8	−0.41	−11.2	1.53	7.7
13	3996	3.3	17.3	0.116	0.512039	9	−0.41	−11.7	1.55	8.3
14	4062	5.4	28.5	0.115	0.512086	25	−0.42	−10.8	1.47	8.9
15	4074	4.7	24.9	0.114	0.512122	20	−0.42	−10.1	1.40	9.0
16	4116	2.9	16.4	0.106	0.511725	12	−0.46	−17.8	1.84	9.4
17	4140	3.0	16.6	0.109	0.511722	19	−0.44	−17.9	1.91	10.0
18	4152	4.7	26.8	0.106	0.511666	19	−0.46	−19.0	1.94	11.9
19	4176	4.7	28.2	0.101	0.511658	12	−0.49	−19.1	1.86	13.2
20	4266	5.3	30.1	0.105	0.511711	18	−0.46	−18.1	1.86	15.1
21	4344	6.2	35.8	0.105	0.511625	17	−0.47	−19.8	1.98	17.0
22	4458	3.7	21.6	0.103	0.511628	18	−0.47	−19.7	1.94	21.1
23	4536	2.4	13.6	0.108	0.511698	79	−0.45	−18.3	1.92	23.0
24	4608	4.8	27.7	0.105	0.511619	17	−0.47	−19.9	1.99	23.4

[a] Assuming $^{143}Nd/^{144}Nd_{today} = 0.512638 (^{146}/^{144}Nd = 0.72190)$; $\varepsilon Nd_{(0)} = (([^{143}Nd^{144}Nd][sample, now] / 0.512638) - 1) \times 10^4$.
[b] Nd Model age after DePaolo (1981).
[c] Stratigraphic ages in Appendix A and data repository 1.

individual groups per sample are presented in Data Repository 2 and discussed in Appendix C. The counts per sample and taxon are listed in Data Repository 3. All results are plotted in diagrams using Tilia 7.6 software (Grimm, 1991) and subdivided into pollen zones based on stratigraphical constrained cluster analysis using the total sum of squares (CONISS: Grimm, 1987; Gill et al., 1993).

A note of caution is warranted concerning the drilling mud. The origin of this mud was of likely North American origin (D. Pocknall, pers. comm) and therefore typical boreal taxa (such as *Alnus*, *Carya*, *Myrica*) were excluded from the interpretation. It also should be noted that preservation of terrestrial material in the submarine fan in general is good (Hoorn, 1997; Haberle, 1997). However, in Well 2 a considerable proportion of pollen is poorly preserved. We suspect this is due to the use of chemicals during drilling and sample storage since drilling. Nevertheless, it does not impede the identification of the transition between biomes.

5.3.2. Taxonomic identification and aggrupation of the taxa

Sporomorphs were classified with the help of palynological catalogues, databases, and the pollen reference collection at the University of Amsterdam (Regali et al., 1974; Lorente, 1986; Roubik and Moreno, 1991; Hoorn, 1993, 1994; Bush and Weng, 2006; Leite, 2006; Jaramillo and Rueda, 2008 (updated in 2016); Jiménez et al., 2008; Silva-Caminha et al., 2010; Jaramillo et al., 2011, 2014).

Pollen rain studies and paleoecological research in northern South America form the basis for the aggrupation of the pollen taxa (Haberle, 1997; Marchant et al., 2002; Weng et al., 2004; Gosling et al., 2009; Moscol-Olivera et al., 2009; Niemann et al., 2009; Burn et al., 2010; Jaramillo et al., 2014; Bogotá-A et al., 2015; Cassino et al., 2015). We used these data to estimate the contribution of the (sporomorph) parent taxa and their corresponding biomes to the FAB record (Appendix B).

We distinguished 14 ecological categories and the composition of each individual group is listed in Appendix B. The current distribution of characteristic biomes in the Amazon drainage basin is shown in Fig. 7. The groups are as follows: 1) mangrove vegetation, 2) tropical lowland forest, 3) tropical lower montane forest, 4) tropical montane forest, 5) tropical forest to savanna, 6) tropical lowland to montane forest, 7) Savanna–*Cerrado*, 8) open Andean vegetation (reflecting *Puna* and *Paramo*), 9) Poaceae, 10) Asteraceae, 11) freshwater communities (tropical lowland), 12) freshwater communities (mainly herbs such as Cyperaceae, *Typha* and associates), 13) 'other elements', including taxa of wide and unknown distribution, and unidentified types, and 14) reworked, corroded or folded sporomorphs (not included in the pollen sum). These groups form the basis for the organization of the palynological data (Fig. 5; Appendix C).

The tropical lowland forest (group 2) generally can be subdivided further into three forest communities: a) Moist evergreen tropical forest with a mean annual temperature ranges from 23 to 27 °C and 2000–4000 mm precipitation per year (UNESCO, 1981); b) Seasonally dry semi-deciduous tropical forests with 700–1600 mm precipitation per year and a marked dry season; and c) *Cerrado* to moist savannas with precipitation ranging between 1000 and 2000 mm per year, a pronounced dry season, and mean annual temperature of 16–25 °C. Our reference for the characteristic composition of lowland vegetation are the studies performed in the Noel Kempff Mercado National Park in northeast Bolivia (Gosling et al., 2009; Burn et al., 2010). This area is situated in southwestern Amazonia and includes a mix of mature moist evergreen tropical forest, semi-deciduous tropical forest and *Cerrado* (well-drained savanna) communities. A detailed characterization of the latter is documented by Cassino et al. (2015) who described different types of *Cerrado* communities in the National Park of Brasilia and the National Park of Grande Sertão Veredas (Brazil).

Poaceae and Cyperaceae occur throughout the drainage basin in a variety of environments ranging from aquatic ecosystems (Piedade et al., 2010) to seasonally inundated savannas within the lowland ecosystems (Burn et al., 2010) and open Andean vegetation (e.g. Van 't Veer and Hooghiemstra, 2000).

The optimum climatic and altitudinal envelope of taxa from the open Andean vegetation gives us interesting clues on the provenance of part of the palynological material in the FAB. Species composition along the altitudinal gradient in the eastern Andes (i.e. mountain forest and *Paramo* vegetation) and southeastern Peru (cloud forest and *Puna*) and their pollen representation are described by Niemann et al. (2009) and Weng et al. (2004), respectively. The climatic envelope for selected key taxa lies between 3200 and 4000 m elevation and is documented in

Please cite this article as: Hoorn, C., et al., The Amazon at sea: Onset and stages of the Amazon River from a marine record, with special reference to Neogene plant turnover in ..., Glob. Planet. Change (2017), http://dx.doi.org/10.1016/j.gloplacha.2017.02.005

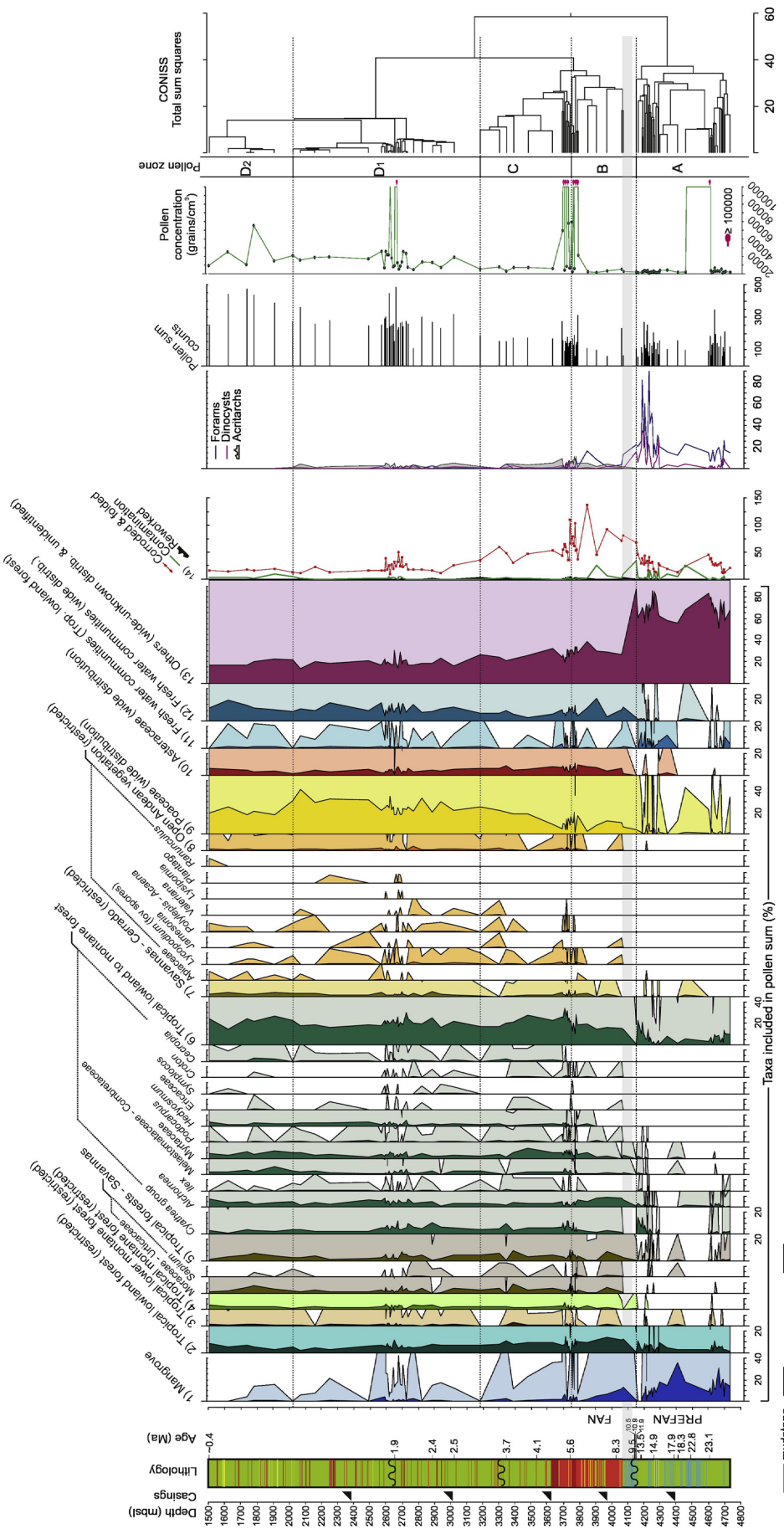

Fig. 5. The palynological summary diagram is based on grouping individual taxa into biomes and is subdivided into 5 zones following CONISS clustering. The zones represent the most important phases of development in terms of arrival of source-indicative pollen types. In dark shades the percentage values, and in light shades the exaggerated values (the exaggeration in all records is x 20, this is to make some of the low percentages better visible).

Please cite this article as: Hoorn, C., et al., The Amazon at sea: Onset and stages of the Amazon River from a marine record, with special reference to Neogene plant turnover in ..., Glob. Planet. Change (2017), http://dx.doi.org/10.1016/j.gloplacha.2017.02.005

Van 't Veer and Hooghiemstra (2000), Weng et al. (2004), Flantua et al. (2014) and Bogotá-A et al. (2015).

6. Results and interpretation

The geochemical and palynological data sets are presented separately because they do not have the same temporal resolution. In the discussion, the data are integrated to give a better understanding on the meaning of the combined results. For Nd isotopes we present the data and their interpretation according to the source area and nannofossil zone, whereas the palynological zones are indicated by pollen zone, nannofossil zone, and the estimated age.

6.1. Geochemistry

The Sm-Nd isotope data for fine-grained rocks collected in Well 2 are presented in Table 1 and based on the age of mineral formation they can be subdivided into two groups (Fig. 4B). The concentration of Sm ranges between 2.9 and 7.5 ppm and Nd varies from 13.6 to 38.8 ppm indicating some degree of variation in the analyzed samples without distinguishing clusters. The observed ratio of $^{143}Nd/^{144}Nd$ ratio ranges from 0.511619 to 0.512200. The values of εNd and T_{DM} range from −8.6 and −19.9 and 1.32 to 1.99 Ga, as well as, the values of $f^{Sm/Nd}$ (−0.40 to −0.49).

The present εNd (0) values and Nd model ages are statistically evaluated with a *t*-test (Table 2). When applying the *t*-test (unpaired parametric analysis) to the εNd value and Nd model age groups, the results are P value = 0.0001 and degree of freedom = 22. The obtained P values are considered to be extremely statistically significant.

6.1.1. Cratonic provenance (NP25-NN10; 23.4–9.4 Ma; latest Oligocene - late Miocene)

The geochemical results from the sediment samples between 4608 and 4116 mbsl (23.4 to 9.4 Ma) suggest T_{DM} from 1.99 to 1.84 Ga and $\varepsilon Nd_{(0)}$ values of −19.9 and −17.8 (Figs. 3 and 4B; Table 1). These samples have a similar geochemical signature as the Urucara, Tapajos and Trombetas rivers (Allègre et al., 1996), which are all tributaries of the Amazon River and exclusively flow across cratonic and reworked Phanerozic sedimentary rocks. Our results are in agreement with Figueiredo et al. (2009) who also analyzed the pre-Fan section. In Fig. 4A we have plotted reference data sets for clay, suspended matter and sedimentary rocks with significant Precambrian contribution (Basu et al., 1990; McDaniel et al., 1997; Figueiredo et al., 2009), which plot in Field I. In Fig. 4B, we plot our own data from the lower Neogene section, which coincide with Field I and suggest a strong contribution of the cratonic and/or reworked Phaneorozoic rocks of the Amazon Craton and platform cover (see Fig. 1A for location).

6.1.2. Andean provenance (NN10-NN19; 9 Ma–1.2 Ma; late Miocene - Pleistocene)

The samples from the interval ranging from 4074 to 2591 mbsl (dated 9 to 1.2 Ma; Figs. 3 and 4B; Table 1) have $\varepsilon Nd_{(0)}$ values and T_{DM} varying from −8.6 to −11.7 and 1.55 to 1.32 Ga, respectively.

Table 2
Mean $Nd_{(0)}$ value and Nd (T_{DM}) model ages of two sample groups from Well-2. SD = standard deviation, SEM = standard error of difference, n = number of samples.

	Fan	pre-Fan
Mean of $\varepsilon Nd_{(0)}$ value	−10.1	−18.8
SD	2.7	0.8
SEM	0.7	0.3
N	15	9
Mean of Nd model age (Ga)	1.47	1.92
SD	0.07	0.05
SEM	0.02	0.02
N	15	9

Such Nd isotope signatures resemble that of suspended matter in the rivers Amazonas, Marañón-Solimões, Beni-Madeira and Rio Negro (Allègre et al., 1996; Hatting, 2014). These rivers receive an important sediment contribution from the Andes (Field III, Fig. 4A) or mixed sources (Field II, Fig. 4A), and this enables us to define a field for sediments or sedimentary rocks with significant contribution of Andes material. Holocene muds and Pliocene to upper Miocene pelitic rocks in the FAB present a similar Nd isotope signal (see McDaniel et al., 1997 and Figueiredo et al., 2009 respectively) (Fig. 4A). The field of the Nd isotope signal for Andean rocks (see Methods section) is highlighted by a black ellipse in Field III of Fig. 4B.

Our data from this period all fall in Field III (Fig. 4B). This means that from late Miocene to present the FAB sediments are of Andean origin, and have an isotope signal that is very similar to the foreland deposits of the Madre de Dios fluvial sands as presented by Basu et al. (1990).

6.2. Palynology

Over 700 sporomorph types were identified in the Well 2 section and grouped according to their ecological preference (Appendix B). The main results are represented in Fig. 5 (Appendix C), but the data are also shown in linear time (Appendix D) and as individual concentration graphs per biome (Appendix E). The palynostratigraphic marker scheme is presented in relation to the nannofossil zonation of Varol Research (2004) (Fig. 6). The palynological results are discussed below and follow the 4 zones that were distinguished based on cluster analysis of the data (Figs. 3 and 5).

6.2.1. Pollen zone A (NN 1-NN 6; 24–12.5 Ma; latest Oligocene - middle Miocene)

This pollen zone includes samples from 4734 to 4164 mbsl. In this zone sedimentation rates are about 4 cm per 1000 year (Figueiredo et al., 2009) and the pollen concentration is below 2000 grains per cm^3 (Fig. 5). Mangrove pollen (group 1) predominate and taxa from the lowland floodplain environment (group 11) are also common. Pollen diversity is high, but mostly unclassified, and is probably sourced in the highly diverse forest of the tropical lowlands. Overall, the combination of coastal plain and flood plain taxa, and the absence of typical Andean pollen taxa are in agreement with the geochemical provenance in the Amazon lowlands. The exclusive occurrence in this zone of biostratigraphic marker species such as *Horniella lunarensis*, *Bombacacidites* aff. *baculatus*, *Rhoipites gigantiporus* and *Lanagiopollis crassa* agree with the age ranges reported in the biostratigraphic zonation of the Llanos Basin (Jaramillo et al., 2011). Instead, *Cyatheacidites annulatus* makes a much earlier appearance here than observed in the Llanos (Fig. 6).

6.2.2. Pollen zone B (NN6 - NN11; 12.5–5.7 Ma; late middle- late Miocene)

This pollen zone includes samples ranging from 4152 to 3756 mbsl. Between 4146 and 4140 mbsl the stratigraphic break occurs, which represents a regional unconformity. The first two palynological samples in this zone are part of what geochemically still is considered as the pre-Fan section.

In this zone sedimentation rates rise to c. 13 cm per 1000 year (Figueiredo et al., 2009), and — except for some outliers at the top of the zone pollen — concentrations remain low. The most remarkable feature of the zone is the onset of open Andean vegetation taxa (group 8) such as *Jamesonia* and *Lycopodium* foveolate spores type (*Huperzia*) (4062 mbsl; 8.8 Ma), followed by *Rubus*, *Galium*, Ericaceae, *Hedyosmum*, *Lophosoria* and *Isoëtes*. This change in sporomorph composition comes after the geochemical change in provenance that is reported between 4116 and 4074 mbsl (9.4–9 Ma). The first occurrence of the high altitude taxon *Polylepis-Acaena* (3768 mbsl onwards; 5.8 Ma) also occurs in this zone. In addition, Poaceae and Asteraceae (groups 9 and 10) increase, and there is a regular occurrence of Moraceae-Urticaceae, *Cerrado* and savanna taxa (group 7), and elements of the fresh water communities (group 12).

Please cite this article as: Hoorn, C., et al., The Amazon at sea: Onset and stages of the Amazon River from a marine record, with special reference to Neogene plant turnover in ..., Glob. Planet. Change (2017), http://dx.doi.org/10.1016/j.gloplacha.2017.02.005

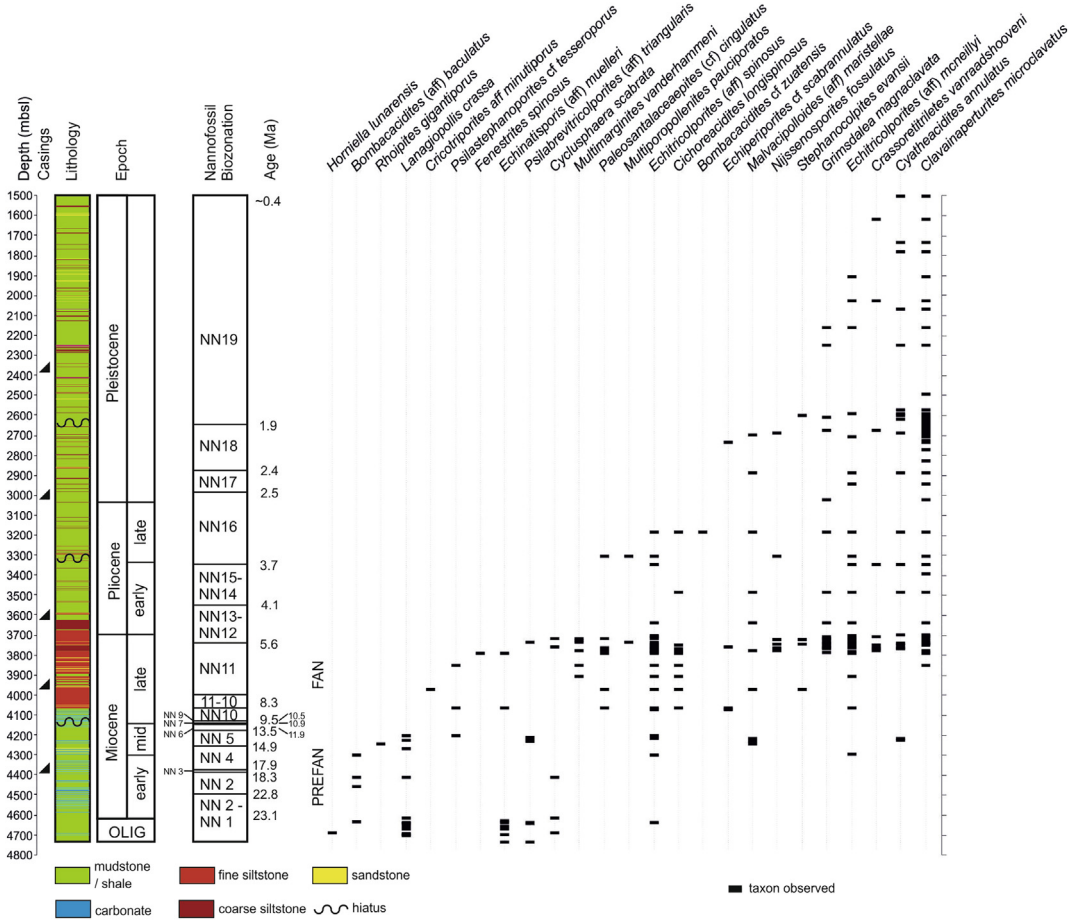

Fig. 6. Palynological marker species in Well 2 in relation to the nannofossil zonation (after Varol Research, 2004).

Like in the previous zone, mangroves (group 1), and tropical lowland taxa (groups 2) remain common, albeit less than in zone A, and there is a drop in taxa from the fluvial floodplains, such as *Mauritia* pollen (group 11).

The exclusive occurrence of biostratigraphic marker species such as *Cricotriporites* aff. *minutiporus* and *Psilastephanoporites* aff. *tesseroporus*, and their position in relation to FAB nannozonation agrees with the biostratigraphic zonation in the Llanos Basin (Jaramillo et al., 2011) (Fig. 6).

6.2.3. Pollen zone C (NN 11–16; 5.7–2.6 Ma; latest Miocene to Pliocene)

This pollen zone includes samples ranging from 3750 to 3185 mbsl. The sedimentation rates and pollen concentration (excluding outliers) both increase, with pollen concentration ranging between 5000 and 10,000 grains per cm^3. Because of the increase in terrestrial input the mangrove pollen and marine palynomorphs sharply dwindle. This zone sees a further rise of the Poaceae, particularly from 3482 mbsl onwards (4 Ma). There are regular occurrences of *Polylepis-Acaena* and a variety of Andean fern taxa. *Valeriana* and *Cecropia*, also make their first appearances (5.4 Ma). *Valeriana* is a typical representative of the high altitude vegetation, whereas *Cecropia* is an Andean taxon that is also common along the Andes-born rivers. This suggests that the high Andes is now an important source area for both sediments and palynological matter. It is unlikely these pollen types came by aerial transport as atmospheric circulation is directed towards the west. Haberle (1997) furthermore reports *Cecropia* as a taxon indicative of second-growth and disturbance, associated with glacial forest taxa. Biostratigraphic marker species such as *Fenestrites spinosus*, *Multimarginites vanderhammenii*, *Multiporopollenites pauciporatus*, *Nijssenosporites fossulatus*, and *Bombacacidites zuatensis* have very late first appearances when compared to their first appearance dates known from the Llanos Basin (Jaramillo et al., 2011) (Fig. 6).

6.2.4. Pollen zone D (NN16 - NN19; 2.6–0.5 Ma; Pleistocene)

This pollen zone includes samples ranging from 3023 to 1502 mbsl. Sedimentation rates are very high, around 1.4 m per 1000 year (Figueiredo et al., 2009) and, with the exclusion of outliers, pollen concentrations rise up to 25,500, with outliers of 55,000 grains per cm^3. The zone is subdivided into two subzones.

Subzone D1 includes samples 3023 to 2024 mbsl and ranges in age from 2.6 up to 0.8 Ma and has very high (20–40%) percentages of Poaceae, accompanied by taxa such as *Lysipomia*, *Plantago*, *Valeriana*, *Polylepis-Acaena*, Caryophyllaceae, *Lachemilla*, *Geranium*, *Hypericum*, *Eringium*, *Lysipomia*, *Aragoa* and others. These are all taxa typical for open vegetation in the high Andes (group 8). At this time the Andes was under the influence of the Quaternary glaciations, which favored an expansion of this vegetation type (Torres et al., 2013; Bogotá-A et al., 2015). This also explains the relative increase of tropical montane taxa, which had the opportunity to expand into the tropical lowlands (Haberle and Maslin, 1999). Biostratigraphic markers such as *Echiperiporites* cf. *scabrannulatus*, *Malvacipolloides* aff. *maristellae*, *Nijssenosporites fossulatus*, and *Stephanocolpites evansii* have their last appearance in this zone (Fig. 6).

Subzone D2 ranges in age from 0.8 to 0.5 Ma. Poaceae and Cyperaceae are the most dominant groups although the Poaceae are less abundant than in the previous zone. Ranunculaceae, a taxon of the open Andean vegetation (group 8), makes its first appearance in this zone whereas *Lysipomia*, *Plantago*, *Valeriana* are not recorded. Biostratigraphic markers of long ranges were observed. Key taxa such as

Alnus and *Quercus* had to be excluded from the biomarker scheme due to contamination from the drilling mud (see Methods section).

7. Discussion

7.1. Regional geology and onset of the transcontinental Amazon River

Our new data from Well 2 suggest that the onset of the transcontinental Amazon River occurred within biostratigraphic zone NN10, between samples dated to 9.4 and 9 Ma. This is 1 to 1.5 million years later than proposed by Figueiredo et al. (2009; corrected to 10.5 Ma in 2010), but in agreement with Dobson et al. (1997 and 2001) and Gorini et al. (2013). Notably, Dobson et al. (1997 and 2001) hinted at a 10–9 Ma onset of the Amazon River based on a geochemical study of samples from the Ceara Rise, a submerged plateau in the western Atlantic. Gorini et al. (2013) propose a 9.5 to 8.3 Ma age bracket (NN10) for the onset of the Amazon River, based on a regional review of seismic data and exploration wells in the FAB. They agree with Pasley et al. (2005) and Figueiredo et al. (2009) that the transcontinental river followed from the combined effect of late Miocene global sea level lowstand and ongoing uplift in the Andes.

Why and how the merging of two previously disconnected aquatic systems, one in eastern Amazonia and the other in western Amazonia (Hoorn, 1994; Wesselingh, 2006; Figueiredo et al., 2009), took place is still unclear. To understand the development of the Amazon River we have to view the new data set into the dynamic geological context of northern South America. The history of northern South America is marked by the opening of the Atlantic (Mora, 2007), oceanic plate break-up and subduction processes along the Pacific margin (Barckhausen et al., 2008; Espurt et al., 2007), tectonism in the Eastern Cordillera (e.g. Horton et al., 2010) and deformation of the Caribbean plate (Farris et al., 2011; Boschman et al., 2014; Montes et al., 2015). These processes are at least in part interconnected and are discussed below.

The first signs of uplift of the Eastern Cordillera (Peru to Colombia) are apparent in the early Oligocene (31 Ma) (Parra et al., 2009; Horton et al., 2010; Ochoa et al., 2012; Eude et al., 2015). There are now several lines of evidence that suggest that in the middle Miocene the Central Andes already reached altitudes of c. 2.5 km (Leier et al., 2013; Cooper et al., 2016), and that the Venezuelan Andes reached similar altitudes by the late Miocene-Pliocene (Bermúdez et al., 2015). The newly formed cordillera also constituted an orographic barrier, and with altitudes of 2000 m it exercised an effective control on climate and induced convective rainfalls (Mulch et al., 2010; Poulsen et al., 2010; Barnes et al., 2012). This must have led to increased water and sediment run-off into the adjacent foreland basins. At least since the early Miocene times fluvial deposits of Andean origin accumulated in western Amazonia (Wesselingh, 2006; Salamanca et al., 2016) and fluvial deposition continued in this region until c. 5 Ma (Latrubesse et al., 2010).

Mountain building in the Andes is intimately related with subsidence and sediment deposition in the Subandean basins (Bayona et al., 2008; Horton et al., 2010; Mora et al., 2010; Roddaz et al., 2010), and it also played a role in the formation of the Amazon drainage basin. Another driver of depositional patterns at continental scales and over million of years is dynamic topography. Mantle convection too might have played a role in the reorganization of drainage patterns and the establishment of the Amazon River (Shephard et al., 2010; Eakin et al., 2014).

Topographic barriers define the delimitations of the Amazon drainage basin, and separate it from neighboring river systems, such as the Orinoco and the Paraná. Mora et al. (2010) observed that the Vaupes Swell (Fig. 1A) only was formed in the late Miocene and constitutes the northern divisor between the Orinoco and Amazon drainage basin. This coincided with subsidence of the Gurupá Arch (Fig. 1A), which opened up a passage towards the Atlantic (Caputo and Soares, 2016). Prior to the late Miocene time the Orinoco and Amazon drainage basins were connected and fluvial deposits from the Caribbean reached western Amazonia (Salamanca et al., 2016). The Fitzcarrald Arch (Fig. 1A) forms the southwestern barrier of the Amazon drainage basin, and was formed as a by-product of the Nazca Plate subduction (Espurt et al., 2007). This arch was uplifted around at 4 Ma (Pliocene) and became a source of sediment influx into the Amazon lowlands.

Another relevant topographic feature in the evolution of the Amazon drainage system is the Purus Arch (Fig. 1). This divisor between the Solimões and Amazonas basins is thought to have acted as a crucial barrier, which until the late Miocene withheld the western drainage from connecting with the eastern half (Figueiredo et al., 2009). However, its role is questionable. In other works it is used as evidence for a Pliocene to mid or even late Pleistocene age of onset for the Amazon River (Nogueira et al., 2013; Horbe et al., 2013; Rossetti et al., 2015). These authors suggest that the Purus Arch could only have breached in the Pleistocene, after deposition of the Içá Formation. The exact meaning of the Purus Arch remains to be resolved, but alternative scenarios, in which drainage circumvents this barrier are feasible.

All this suggests that the formation of the Amazon drainage basin was a complex geological process that initiated with mountain building in the Eastern Cordillera in the Oligocene, and was completed during the late Miocene and early Pliocene with formations of barriers that confined the Amazon drainage basin into its present state.

Regional geological change in the northern Andes not only affected the build-up of the Amazon Fan, but also left its marks in the Caribbean Sea. Records from ODP leg 165 show large-scale changes in sediment deposition and composition following the uplift of Hispaniola, Guatemala, and the Northern Andes (Peters et al., 2000). This further emphasizes the extent and magnitude of the geological deformation in northern South America and its effect on fluvial and even marine systems. Furthermore, it would fit well in the context of the 'old' Panama model, which suggests a middle Miocene closure of the Central American Seaway following regional tectonism (Farris et al., 2011; Montes et al., 2015), but evidence is debated (see O'Dea et al., 2016).

7.2. Climatic change and its influence on the Amazon drainage basin

The effects of climate and tectonism are difficult to disentangle in the sedimentary record. On global scale, and particularly from late Pliocene onwards, erosion rates have significantly increased and such changes were previously attributed to mountain uplift, however Molnar and England (1990) and Molnar (2004) proposed that climate change was the real cause of this. In recent years the role of the Plio-Pleistocene climatic variations on erosion rates was accepted as main driving force and responsible for most of the modern relief (e.g. Herman et al., 2013; Herman and Champagnac, 2015).

Harris and Mix (2002) highlight the role of long-term erosion and climate change in tropical South America based on the clay geochemistry of a 13 million year record at Ceara Rise. They suggest that between 8 and 4.5 Ma the Amazon drainage basin expanded into a more arid zone. This coincides with the western Amazonia changing from an extensive fluvio-lacustrine wetland system into a fully fluvial system (Hoorn et al., 2010; Latrubesse et al., 2010; Silva-Caminha et al., 2010). Our results further suggest that between 9.4 and 9 Ma the proto-Amazon River in eastern Amazonia transformed into a transcontinental river (see also Figueiredo et al., 2009; Caputo and Soares, 2016).

The Plio-Pleistocene climatic transition and global sea level lowstand mark the final stages in the development of the Amazon drainage basin. In the Bolivian Andes rapid alluvial canyon incision occurs during the early Pliocene (Lease and Ehlers, 2013), while in the Subandean zone megafan systems develop that extend into western Amazonian (Wilkinson et al., 2010). In addition, the newly formed Fitzcarrald Arch (Espurt et al., 2007) (Fig. 1) starts acting as a new sediment source area. Meanwhile, the Amazon River and its tributaries start carving deep channels into the bedrock (Irion and Kalliola, 2010) and becomes a giant conveyor system that discharges vast amounts of Andean sediments

Please cite this article as: Hoorn, C., et al., The Amazon at sea: Onset and stages of the Amazon River from a marine record, with special reference to Neogene plant turnover in ..., Glob. Planet. Change (2017), http://dx.doi.org/10.1016/j.gloplacha.2017.02.005

into the ocean. In the Amazon submarine fan this leads up to the main phase of sediment build up (Flood et al., 1995; Flood and Piper, 1997). Undeniably, the late Pliocene and Quaternary climatic variations caused large geographic changes, which explains why some see it as the true age of onset of the Amazon River (Campbell et al., 2006; Horbe et al., 2013; Rossetti et al., 2005, 2015).

Climate change, intense erosion, and a changing landscape in the Andes-Amazonian system all must have contributed to the emergence of new plant biomes in the Andes and the Amazon lowlands. The increase in grasses observed in our section (Figs. 3 and 5 and Appendix D) from late Miocene to Pleistocene coincides with this period of large continental change. Grasses may well had an advantage and as pioneering vegetation they may have colonized the landslide surfaces and megafans in the Subandean zone. Furthermore, the incised river valleys, reduced floodplains in the Amazon lowlands, and an extensive coastal shelf possibly led to the formation of savanna and *Cerrado* biomes.

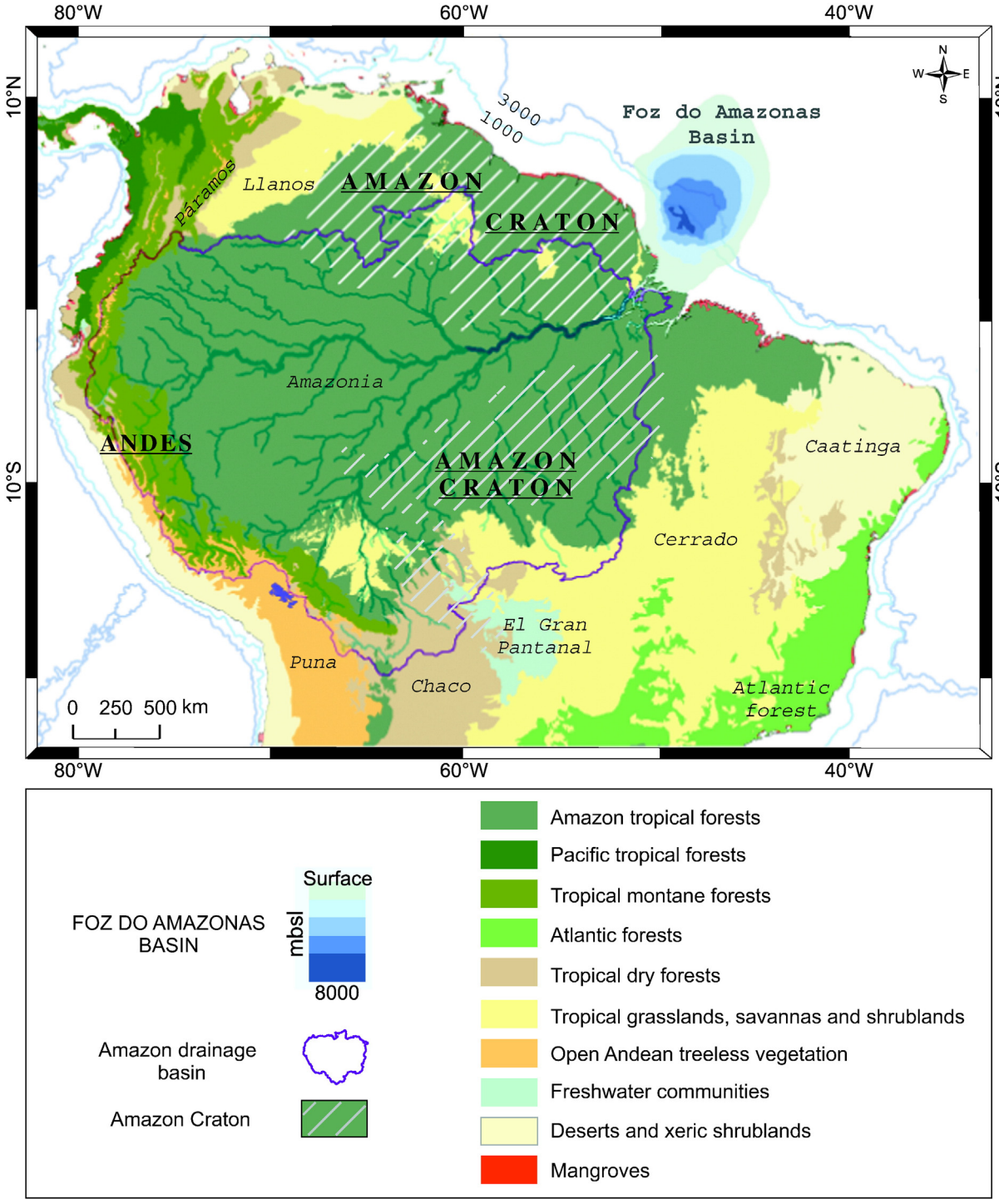

Fig. 7. The distribution of biomes or vegetation units in northern South America, including the Amazon drainage basin and peripheral areas. This map illustrates (like Fig. 1A does for the geochemistry) what the source area for the palynological matter may have been. Data sources: Foz do Amazonas Basin modified from Wanderley-Filho et al. (2010); Ecoregion map modified from Olson et al. (2001); Hydrology from Mayorga et al. (2012).

Please cite this article as: Hoorn, C., et al., The Amazon at sea: Onset and stages of the Amazon River from a marine record, with special reference to Neogene plant turnover in ..., Glob. Planet. Change (2017), http://dx.doi.org/10.1016/j.gloplacha.2017.02.005

7.3. A late Miocene biotic turnover in the Amazon drainage basin

On global scale, the Neogene is an important time interval for grassland development and characterized by the emergence of C4-type grasses, typically forming the tropical and subtropical grasslands and savannas (Jacobs et al., 1999; Strömberg, 2011). In our Neogene FAB record the grasses form one of the most remarkable palynological groups (Fig. 5). It is, however, difficult to be sure of their exact provenance. There are several candidate source areas (Fig. 7), ranging from the open vegetation in the high Andes to the tropical lowland savannas and *Cerrado*, the floating meadows or river floodplains, or a combination of some or all of these. We evaluate below which is the most plausible scenario.

In our data set Poaceae, Cyperaceae, *Typha*, and other taxa of the fresh water communities (group 12), all rise in the late Miocene (from 9 Ma). This time frame agrees with the global onset of savannas that is dated at 9 Ma (Beerling and Osborne, 2006). The Poaceae gradually increase further and become dominant at 4 Ma, which agrees with estimates from molecular phylogenetic studies that point at an onset of the *Cerrado* biome around c. 4 Ma, and further expansion at 2.3 Ma (Simon et al., 2009; Simon and Pennington, 2012). In the Amazon Fan section, Poaceae reach percentages well above postglacial and modern values between 2.6 and 0.8 Ma the. Noticeably, this is the first evidence of a basin-wide expansion of the grasslands during the Plio-Pleistocene transition in the Amazon drainage basin.

The question remains, how can the main contributing source of grass pollen to the FAB be identified? We contemplate here the different scenarios. One possibility is that floating meadows and grasslands associated to the Amazon River are the principal source. Such meadows and grasslands are very common in the lower reaches of the Amazon River (Absy et al., 2014: Cassino et al., 2015) and grass pollen are known to be abundant in water samples from this area (Haberle, 1997). However, it should be noted that the entire Amazon drainage basin covers an area of 6.068.562 km^2 (Seyler et al., 2009), and that lowland savannas (2.297.432 km^2) and highland grasslands (2.354.544 km^2) form over two thirds of the drainage basin and are thus likely to have a large share in the pollen contribution. This makes it unlikely that the lower reaches of the river would have been the main cause of the rise of the grasses. Particularly since this area was already drained by the proto-Amazon River before the rise of the grasses started.

Another possible scenario is that the grasses increased at the expense of other vegetation types, such as the lowland rainforest. Could it, for instance, be that they occupied the newly formed habitats on the dried-up lakes and floodplains of the Pebas System in western Amazonia, or expanded from the *Cerrado*? To assess this further we compared the concentration values of the palynological group across time (Appendix E). We observe that tropical lowland taxa remained relatively constant throughout the late Miocene to Pleistocene, and that the increase in grass pollen is accompanied by an increase in taxa from the tropical montane forest (groups 3, 4, 6), *Cerrado* and savanna (group 7), open Andean vegetation (group 8), Asteraceae (group 10), and the fresh water communities (group 12). This suggests that the tropical lowland forest did not significantly loose terrain in favor of grass expansion. Altogether this suggests that the increase of the grass pollen in the FAB was a basin-wide phenomenon, but most likely took place in the upper reaches of the drainage basin.

The sediment geochemistry in the Plio-Pleistocene Amazon Fan section, and the vast increase in sedimentation rates further imply that the Andes was the principal sediment source area during this time. This prompts us to believe that the open, treeless Andean vegetation (*Páramo* and *Puna*; Fig. 7), and possibly pioneering vegetation on the megafans in the foothills might have been the greatest contributor of grass pollen into the FAB. This is consistent with data from Plio-Pleistocene biomarker records in the high Andes, which document the transition of C3 grasses to the invasive, C4 grasses, that typically form the modern grasslands (e.g. Boom et al., 2001). Nevertheless, this matter can be definitively resolved with further high-resolution microscopy studies of the grass pollen, and possibly phytoliths, in the Neogene FAB record.

8. Conclusions

The Neogene section in the Foz do Amazonas forms a very important record in which both palynological and geochemical analysis allowed us to, unequivocally, determine the provenance history of the Amazon River. We used this combined approach to re-address the debate on the age of the onset of the transcontinental Amazon River. We conclude that that the transition from a river born in the tropical lowlands to a transcontinental river occurs between 9.4 and 9 Ma. At least from 9 Ma onwards the characteristic Andes-dominated geochemical signature reaches the Atlantic. This age can be taken as a minimum for the onset of the transcontinental river that connected the Andes to the Atlantic and narrows down the age bracket from previous estimates (Dobson et al., 2001; Figueiredo et al., 2009; Gorini et al., 2013). Notably, the onset of the river post-dates by 1 to 1.5 My the regional unconformity.

This marine section also provided an excellent opportunity to assess overall changes in pollen source areas in the drainage basin. The palynological data are in good agreement with the geochemical data and provide further detail on the composition of the terrestrial biomes in the basin. In the Andes a high montane forest already existed in the late Miocene (c. 9 Ma) and, at least from 5.4 Ma onwards, open Andean treeless areas above 2700–3500 m (*Páramos* and *Punas*) occurred. This open Andean treeless vegetation included ferns such as *Jamesonia* and *Huperzia*, and angiosperms with *Polylepis-Acaena* and particularly *Valeriana*, *Lysipomia* and *Plantago*. All these taxa currently have their optimal conditions at altitudes between 3200 and 4000 m asl.

The onset of the Amazon transcontinental river was driven by Neogene tectonics in northern South America and further determined by late Neogene climatic fluctuations. This process facilitated the connection between previously independent drainage systems in eastern and western Amazonia. The large paleoenvironmental changes associated with the development of the drainage basin opened up new habitats, and –in addition to climate change –enabled expansion of pioneering grasses and other herbs.

The late Miocene to Pleistocene record in Foz do Amazonas suggests that in its early stages the drainage system had its source in a forest-dominated tropical lowland and – around 9 Ma – the proto-Amazon River connected with the (high) Andes. By that time the tropical lowland was formed by forest, savanna and *Cerrado*. Between 9 and 4 Ma the grasslands gradually increased. Notably, between 2.6 and 0.8 Ma grass pollen percentages are well beyond modern levels and suggest grassland expansion in the Amazon drainage basin.

In summary, our study shows that major abiotic and biotic changes occurred in the Andes-Amazonian system during the late Neogene. Nevertheless, it will still require extensive further study and explorative effort in the Amazon drainage basin to better understand how exactly biota developed following geological and climatic changes. Transcontinental drilling in this basin (see Baker et al., 2015) may help us to improve further our understanding of the history of the Amazon drainage basin and how biota responded to climatic change from late Miocene onwards.

Supplementary data to this article can be found online at http://dx.doi.org/10.1016/j.gloplacha.2017.02.005.

Data repository

1. Overview of recalculated ages for palynological and geochemical samples (based on Gradstein et al., 2012). https://figshare.com/s/bb28bdbc61f24cd9b7be.

Please cite this article as: Hoorn, C., et al., The Amazon at sea: Onset and stages of the Amazon River from a marine record, with special reference to Neogene plant turnover in ..., Glob. Planet. Change (2017), http://dx.doi.org/10.1016/j.gloplacha.2017.02.005

2. Datasheet with the percentages of the taxa in the ecological groups counted in the samples from Well 2 (see also Methods section). https://figshare.com/s/db6b329536f00fbe00fc.
3. Datasheet with the sample depth and the raw counts of the sporomorph taxa. [In Figshare. Under embargo. Data can be solicited to the authors].

Acknowledgements

This project was developed in the context of the Clim-Amazon program, the joint Brazilian-European facility for climate and geodynamic research on the Amazon River Basin sediment under the European Union's Seventh Framework Program (FP7/2007-2013)/ERC grant agreement no. 226600. E.L acknowledges the Universidade de Brasília (grant 295091) and S.G.A.F. acknowledges NWO (grant 2012/13248/ALW). We acknowledge the Brazilian Oil and Gas Agency (ANP) for permission to publish Well 2 data and seismic section (SID #31404 ANP/UnB). We thank Petrobras for facilitating the samples and the technical discussions with Roberto D'Avila, Emilson Soares, Otaviano Neto. Jorge Figueiredo and Paulus van der Ven are warmly thanked for initiating the cooperation Petrobras-UvA. We are also grateful to Annemarie Philip (University of Amsterdam) for processing the palynological samples, David Pocknall, Stephen Lowe, Jose-Abel Flores and Mark Pasley for valuable discussions, and Henry Hooghiemstra and Martin Roddaz for critical comments on an earlier version of this manuscript. We are very grateful to Carlos Jaramillo and an anonymous reviewer for their constructive comments and review.

References

Absy, Ml, Cleef, A.M., D'Apolito, C., da Silva, M.F.F., 2014. Palynologycal differentiation of savanna types in Carajás, Brazil (southeastern Amazonia). Palynology 38 (1), 78–89.

Allègre, C.J., Dupré, B., Négrel, P., Gaillerdet, J., 1996. Sr-Nd-Pb isotope systematics in Amazon and Congo River systems: constraints about erosion processes. Chem. Geol. 131 (1–4), 93–112.

Baker, P.A., Fritz, S.C., Silva, C.G., Rigsby, C.A., Absy, M.L., Almeida, R.P., Caputo, M., Chiessi, C.M., Cruz, F.W., Dick, C.W., Feakins, S.J., Figueiredo, J., Freeman, K.H., Hoorn, C., Jaramillo, C., Kern, A.K., Latrubesse, E.M., Ledru, M.P., Marzoli, A., Myrbo, A., Noren, A., Piller, W.E., Ramos, M.I.F., Ribas, C.C., Trinadade, R., West, A.J., Wahnfried, I., Willard, D.A., 2015. Trans-Amazon Drilling Project (TADP): origins and evolution of the forests, climate, and hydrology of the South American tropics. Sci. Drill. 20, 41–49.

Barckhausen, U., Ranero, C.R., Cande, S.C., Engels, M., Weinrebe, W., 2008. Birth of an intraoceanic spreading center. Geology 36 (10):767–770. http://dx.doi.org/10.1130/G25056A.1.

Barnes, J.B., Ehlers, T.A., Insel, N., McQuarrie, N., Poulsen, C.J., 2012. Linking orography, climate, and exhumation across the central Andes. Geology 40 (12):1135–1138. http://dx.doi.org/10.1130/g33229.1.

Basu, A.R., Sharma, M., DeCelles, P.G., 1990. Nd, Sr-isotopic provenance and trace element geochemistry of Amazonian foreland basin fluvial sands, Bolivia and Peru: implications for ensialic Andean orogeny. Earth Planet. Sci. Lett. 100, 1–17.

Bayona, G., Cortes, M., Jaramillo, C., Ojeda, G., Aristizabal, J., Reyes-Harker, A., 2008. An integrated analysis of an orogen-sedimentary basin pair: latest Cretaceous–Cenozoic evolution of the linked Eastern Cordillera orogen and the Llanos foreland basin of Colombia. Geol. Soc. Am. Bull. 120, 1171–1197.

Beaudouin, C., Dennielou, B., Melki, T., Guichard, F., Kallel, N., Berné, S., Huchon, A., 2004. The Late-Quaternary climatic signal recorded in a deep-sea turbiditic levee (Rhône Neofan, Gulf of Lions, NW Mediterranean): palynological constraints. Sediment. Geol. 172:85–97. http://dx.doi.org/10.1016/j.sedgeo.2004.07.008.

Beerling, D.J., Osborne, C.P., 2006. The origin of the savanna biome. Glob. Chang. Biol. 12: 2023–2031. http://dx.doi.org/10.1111/j.1365-2486.2006.01239.x.

Bermúdez, M.A., Hoorn, C., Bernet, M., Carrillo, E., van der Beek, P.A., Garver, J.I., Mora, J.L., Mehrkian, K., 2015. The detrital record of late Miocene to Pliocene surface uplift and exhumation of the Venezuelan Andes in the Maracaibo and Barinas foreland basins. Basin Res. 1–26. http://dx.doi.org/10.1111/bre.12154.

Bogotá-A, R.G., Hooghiemstra, H., Berrio, J.C., 2015. North Andean environmental and climatic change at orbital to submillennial time-scales: vegetation, water-levels and sedimentary regimes from Lake Fúquene between 284 and 130 ka. Rev. Palaeobot. Palynol. 226:91–107. http://dx.doi.org/10.1016/j.revpalbo.2015.09.007.

Boom, A., Mora, G., Cleef, A.M., Hooghiemstra, H., 2001. High altitude altitude C4 grasslands in the northern Andes: relicts from glacial conditions? Rev. Palaeobot. Palynol. 115:147–160. http://dx.doi.org/10.1016/S0034-6667(01)00056-2.

Boschman, L.M., van Hinsbergen, D.J.J., Torsvik, T.H., Spakman, W., Pindell, J.L., 2014. Kinematic reconstruction of the Caribbean region since the Early Jurassic. Earth Sci. Rev. 138 (102):102–136. http://dx.doi.org/10.1016/j.earscirev.2014.08.007.

Brandão, J.A.S.L., Feijó, F.J., 1994. Bacia da Foz do Amazonas. Boletim de Geociências da Petrobras 8 (1), 91–99.

Burn, M.J., Mayle, F.E., Killeen, T.J., 2010. Pollen-based differentiation of Amazonian rainforest communities and implications for lowland palaeoecology in Tropical South America. Palaeogeogr. Palaeoclimatol. Palaeoecol. 295:1–18. http://dx.doi.org/10.1016/j.palaeo.2010.05.009.

Bush, M.B., Weng, Ch., 2006. Introducing a new (freeware) tool for palynology. J. Biogeogr. 34:377–380. http://dx.doi.org/10.1111/j.1365-2699.2006.01645.x.

Campbell, A.E., 2005. Shelf-geometry response to changes in relative sea level on a mixed carbonate–siliciclastic shelf in the Guyana Basin. Sediment. Geol. 175 (1–4):259–275. http://dx.doi.org/10.1016/j.sedgeo.2004.09.003.

Campbell, K.E., 2010. Late Miocene onset of the Amazon River and the Amazon deep-sea fan: evidence from the Foz do Amazonas Basin: comment. Geology 38 (7), e212. http://dx.doi.org/10.1130/G30633C.1.

Campbell, K.E., Frailey, C.D., Romero-Pittman, L., 2006. The Pan-Amazonian Ucayali Peneplain, late Neogene sedimentation in Amazonia and the birth of modern Amazon River system. Palaeogeogr. Palaeoclimatol. Palaeoecol. 239:166–219. http://dx.doi.org/10.1016/j.palaeo.2006.01.020.

Caputo, M.V., Soares, E.A.A., 2016. Eustatic and tectonic change effects in the reversion of the transcontinental Amazon River drainage system. Braz. J. Geol. 46 (2):301–328. http://dx.doi.org/10.1590/2317-4889201620160066.

Cassino, R.F., Martinho, C.T., da Silva Caminha, S.A.F., 2015. Modern pollen spectra of the Cerrado vegetation in two national parks of Central Brazil, and implications for interpreting fossil pollen records. Rev. Palaeobot. Palynol. 223:71–86. http://dx.doi.org/10.1016/j.revpalbo.2015.09.002.

Cobbold, P.R., Mourgues, R., Boyd, K., 2004. Mechanism of thin-skinned detachment in the Amazon Fan: assessing the importance of fluid overpressure and hydrocarbon generation. Mar. Pet. Geol. 21:1013–1025. http://dx.doi.org/10.1016/j.marpetgeo.2004.05.003.

Cooper, F.J., Adams, B.A., Blundy, J.D., Farley, K.A., McKeon, R.E., Ruggiero, A., 2016. Aridity-induced Miocene canyon incision in the Central Andes. Geology 44 (8):675–678. http://dx.doi.org/10.1130/G38254.1.

Cordani, U., Sato, K., 1999. Crustal evolution of the South American Platform, based on Nd isotopic systematics on granitoid rocks. Episodes 22 (3), 167–173.

Damuth, J., Kumar, N., 1975. Amazon cone: morphology, sediments, age, and growth pattern. GSA Bull. 6:863–878. http://dx.doi.org/10.1130/0016-7606(1975)86<863:ACMSAA>2.0.CO;2.

Davidson, E.A., Artaxo, P., 2004. Globally significant changes in biological processes of the Amazon Basin: results of the large-scale biosphere–atmosphere experiment. Glob. Chang. Biol. 10 (5):519–529. http://dx.doi.org/10.1111/j.1529-8817.2003.00779.x.

DePaolo, D.J., 1981. A neodymium and strontium isotopic study of the Mesozoic calc-alkaline granitic batholiths of the Sierra Nevada and Peninsular Ranges, California. J. Geophys. Res. 86, 10470–10488.

DePaolo, D.J., 1988. Neodymium Isotope Geochemistry. An Introduction. Springer-Verlag, Berlin (187 pp).

Dobson, D.M., Dickens, G.R., Rea, D.K., 1997. Terrigenous sedimentat Ceara Rise. In: Shackleton, N.J., Curry, W.B., Richter, C., Bralower, T.J. (Eds.), Proceeding of the Ocean Drilling Program, Scientific Results. 154. Ocean Drilling Program, College Station, TX (465–473 pp).

Dobson, D.M., Dickens, G.R., Rea, D.K., 2001. Terrigenous sediment on Ceara Rise: a Cenozoic record of South American orogeny and erosion. Palaeogeogr. Palaeoclimatol. Palaeoecol. 165:215–229. http://dx.doi.org/10.1016/S0031-0182(00)00161-9.

Driscoll, N.W., Karner, G.D., 1994. Flexural deformation due to Amazon Fan loading: a feedback mechanism affecting sediment delivery to margins. Geology 22 (11):1015–1018. http://dx.doi.org/10.1130/0091-7613(1994)022<1015:FDDTAF>2.3.CO;2.

Eakin, C.M., Lithgow-Bertelloni, C., Dávila, F.M., 2014. Influence of Peruvian flat-subduction dynamics on the evolution of Western Amazonia. Earth Planet. Sci. Lett. 404, 250–260.

Encyclopedia Britannica, 2016. Definition of the Amazon River. http://www.britannica.com/place/Amazon-River (28th of April, 2016).

Espurt, N., Baby, P., Brusset, S., Roddaz, M., Hermoza, W., Regard, V., Antoine, P.-O., Salas-Gismondi, R., Bolaños, R., 2007. How does the Nazca Ridge subduction influence the modern Amazonian foreland basin? Geology 35 (6):515–518. http://dx.doi.org/10.1130/G23237A.1.

Eude, A., Roddaz, M., Brichau, S., Brusset, S., Calderon, Y., Baby, P., Soula, J.C., 2015. Controls on timing of exhumation and deformation in the Northern Peruvian Eastern Andean wedge as inferred from low-temperature thermochronology and balanced cross-section. Tectonics 34 (4):715–730. http://dx.doi.org/10.1002/2014TC003641.

Farris, D.W., Jaramillo, C., Bayona, G., Restrepo-Moreno, S.A., Montes, C., Cardona, A., Mora, A., Speakman, R.J., Glascock, M.D., Valencia, V., 2011. Fracturing of the Panamanian Isthmus during initial collision with South America. Geology 39 (11), 1007–1010.

Figueiredo, J., Zalan, P., Soares, E., 2007. Bacia da Foz do Amazonas. Boletim de Geociências da Petrobras 15, 299–309.

Figueiredo, J., Hoorn, C., van der Ven, P., Soares, E., 2009. Late Miocene onset of the Amazon River and the Amazon deep-sea fan: evidence from the Foz do Amazonas basin. Geology 37:619–622. http://dx.doi.org/10.1130/G25567A.1.

Figueiredo, J., Hoorn, C., van der Ven, P., Soares, E., 2010. Late Miocene onset of the Amazon River and the Amazon deep-sea fan: evidence from the Foz do Amazonas basin: REPLY. Geol. Forum 38, 213.

Flantua, S.G.A., Hooghiemstra, H., van Boxel, J.H., Cabrera, M., González-Carranza, Z., González-Arango, C., 2014. Connectivity dynamics since the Last Glacial Maximum in the northern Andes: a pollen-driven framework to assess potential migration. In: Stevens, W.D., Montiel, O.M., Raven, P.H. (Eds.), Paleobotany and Biogeography: A Festschrift for Alan Graham in His 80th Year. Monographs in systematic botany from the Missouri Botanical Garden 128. Missouri Botanical Garden Press, St. Louis, pp. 98–123.

Flood, R.D., Piper, D.J.W., 1997. Amazon fan sedimentation: the relationship to equatorial climate change, continental denudation, and sea-level fluctuations. In: Flood, R.D., Piper, D.J.W., Klaus, A., Peterson, L.C. (Eds.), Proceedings of the Ocean Drilling Program, Scientific Results. 155.

Please cite this article as: Hoorn, C., et al., The Amazon at sea: Onset and stages of the Amazon River from a marine record, with special reference to Neogene plant turnover in ..., Glob. Planet. Change (2017), http://dx.doi.org/10.1016/j.gloplacha.2017.02.005

Flood, R.D., Piper, D.J.W., Shipboard Scientific Party, 1995. Introduction. In: Flood, R.D., Piper, D.J.W., Klaus, A., et al. (Eds.), Proceedings of the Ocean Drilling Program, Initial Reports. 155. http://dx.doi.org/10.2973/odp.proc.ir.155.101.1995.

Gibbs, R.J., 1967. The geochemistry of the Amazon river system: part I. The factors that control the salinity and the composition and concentration of the suspended solids. GSA Bull. 78, 1203–1232.

Gill, D., Shomrony, A., Fligelman, H., 1993. Numerical zonation of the log suites and logfacies recognition by multivariate clustering. AAPG Bull. 77, 1781–1791.

Gioia, S.M.C.L., Pimentel, M.M., 2000. The Sm-Nd isotopic method in the geochronology laboratory of the University of Brasília. An. Acad. Bras. Cienc. 72:219–245. http://dx.doi.org/10.1590/S0001-37652000000200009.

Gorini, C., Haq, B.U., dos Reis, A.T., Silva, C.G., Cruz, A., Soares, E., Grangeon, D., 2013. Late Neogene sequence stratigraphic evolution of the Foz do Amazonas Basin, Brazil. Terra Nova 26 (3):179–185. http://dx.doi.org/10.1111/ter.12083.

Gosling, W.D., Mayle, F.E., Tate, N.J., Killeen, T.J., 2009. Differentiation between Neotropical rainforest, dry forest, and savannah ecosystems by their modern pollen spectra and implications for the fossil pollen record. Rev. Palaeobot. Palynol. 153:70–85. http://dx.doi.org/10.1016/j.revpalbo.2008.06.007.

Gradstein, F.M., Ogg, J.G., Hilgen, F.J., 2012. On the geologic time scale. Newsl. Stratigr. 45 (2):171–188. http://dx.doi.org/10.1127/0078-0421/2012/0020.

Grimm, E.C., 1987. CONISS: a FORTRAN 77 program for stratigraphically constrained cluster analyses by the method of incremental sum of squares. Comput. Geosci. 13:13–35. http://dx.doi.org/10.1016/0098-3004(87)90022-7.

Grimm, E.C., 1991. TILIA and TILIAGRAPH. Illinois State Museum, Springfield.

Haberle, S., 1997. Upper Quaternary vegetation and climate history of the Amazon Basin: correlating marine and terrestrial pollen records. In: Flood, R.D., Piper, D.J.W., Klaus, A., Peterson, L.C. (Eds.), Proceedings of the Ocean Drilling Program, Scientific Results. 155, pp. 381–396.

Haberle, S., Maslin, M.A., 1999. Late Quaternary Vegetation and climate changes in the Amazon basin based on a 50,000 year pollen record from the Amazon Fan ODP Site 932. Quat. Res. 51, 27–38.

Harris, S.E., Mix, A.C., 2002. Climate and tectonic influences on continental erosion of tropical South America, 0–13 Ma. Geology 30 (5):447–450. http://dx.doi.org/10.1130/0091-7613(2002)030<0447:CATIOC>2.0.CO;2.

Hatting, K., 2014. Composição dos isótopos de Sr e Nd nos sedimentos em suspensão da Bacia Amazônica: Implicações para a origem e transporte de sedimentos. M. Sc. Thesis. Universidade de Brasília, Brasília (74 pp).

Heinrich, S., Zonneveld, K.A.F., 2013. Influence of the Amazon River development and construction of the Central American Seaway on Middle/Late Miocene oceanic conditions at the Ceara Rise. Palaeogeogr. Palaeoclimatol. Palaeoecol. 386, 599–606.

Herman, F., Champagnac, J.-D., 2015. Plio-Pleistocene increase of erosion rates in mountain belts in response to climate change. Terra Nova 28 (1), 2–10.

Herman, F., Seward, D., Valla, P.G., Carter, A., Kohn, B., Willett, S.D., Ehlers, T.A., 2013. Worldwide acceleration of mountain erosion under a cooling climate. Nature 504: 423–426. http://dx.doi.org/10.1038/nature12877.

Heusser, L., 1988. Pollen distribution in marine sediments on the continental margin off northern California. Mar. Geol. 80:131–147. http://dx.doi.org/10.1016/0025-3227(88)90076-X.

Hoorn, C., 1993. Marine incursions and the influence of Andean tectonics on the Miocene depositional history of northwestern Amazonia: results of a palynostratigraphic study. Palaeogeogr. Palaeoclimatol. Palaeoecol. 105:267–309. http://dx.doi.org/10.1016/0031-0182(93)90087-Y.

Hoorn, C., 1994. Fluvial palaeoenvironments in the intracratonic Amazonas Basin (Early Miocene-early Middle Miocene, Colombia). Palaeogeogr. Palaeoclimatol. Palaeoecol. 109:1–54. http://dx.doi.org/10.1016/0031-0182(94)90117-1.

Hoorn, C., 1997. Palynology of the Pleistocene glacial/interglacial cycles of the Amazon Fan (holes 940A, 944A, and 946A). In: Flood, R.D., Piper, D.J.W., Klaus, A., Peterson, L.C. (Eds.), Proceedings of the Ocean Drilling Program. Scientific Results. 155, pp. 397–409.

Hoorn, C., Guerrero, J., Sarmiento, G.A., Lorente, M.A., 1995. Andean tectonics as a cause for changing drainage patterns in Miocene northern South America. Geology 23: 237–240. http://dx.doi.org/10.1130/0091-7613(1995)023<0237:ATAACF>2.3.CO;2.

Hoorn, C., Wesselingh, F.P., ter Steege, H., Bermúdez, M.A., Mora, A., Sevink, J., Sanmartín, I., Sanchez-Meseguer, A., Anderson, C.L., Figueiredo, J.P., Jaramillo, C., Riff, D.D., Negri, F.R., Hooghiemstra, H., Lundberg, J., Stadler, T., Särkinen, T., Antonelli, A., 2010. Amazonia through time: Andean uplift, climate change, landscape evolution and biodiversity. Science 330:927–931. http://dx.doi.org/10.1126/science.1194585.

Horbe, A.M.C., Motta, M.B., de Almeida, C.M., Dantas, E.L., Vieira, L.C., 2013. Provenance of Pliocene and recent sedimentary deposits in western Amazônia, Brazil: consequences for the paleodrainage of the Solimões-Amazonas River. Sediment. Geol. 296:9–20. http://dx.doi.org/10.1016/j.sedgeo.2013.07.007.

Horton, B.K., Parra, M., Saylor, J.E., Nie, J., Mora, A., Torres, V., Stockli, D.F., Strecker, M.R., 2010. Resolving uplift of the northern Andes using detrital zircon age signatures. GSA Today 20 (7):4–10. http://dx.doi.org/10.1130/GSATG76A.1.

Irion, G., Kalliola, R., 2010. Fluvial landscape evolution in lowland Amazonia during the Quaternary. In: Hoorn, C., Wesselingh, F. (Eds.), Amazonia, Landscape and Species Evolution, a Look into the Past. Wiley-Blackwell, pp. 185–197.

Jacobs, B.F., Kingston, J.D., Jacobs, L.L., 1999. The origin of grass-dominated ecosystems. Ann. Mo. Bot. Gard. 86 (2), 590–643.

Jaramillo, C.A., Rueda, M., 2008. A morphological electronic database of Cretaceous-Tertiary fossil pollen and spores from northern South America. Colombian Petroleum Institute & Smithsonian Tropical Research (Available at:). http://biogeodb.stri.si.edu/jaramillo/palynomorph/ (Consulted in 2013 and 2014 as version '2008').

Jaramillo, C., Rueda, M., Torres, V., 2011. A palynological zonation for the Cenozoic of the Llanos and Llanos foothills of Colombia. Palynology 35:46–84. http://dx.doi.org/10.1080/01916122.2010.515069.

Jaramillo, C., Moreno, E., Ramírez, V., da Silva, S., de la Barrera, A., Sánchez, C., Morón, S., Herrera, F., Escobar, J., Koll, R., Manchester, S.R., Hoyos, N., 2014. Palynological record of the last 20 Million years in Panama. In: Stevens, W.D., Montiel, O.M., Raven, P. (Eds.), Paleobotany and Biogeography: A Festschrift for Alan Graham in His 80th Year. Monographs in systematic botany from the Missouri Botanical Garden 128. St. Louis: Missouri Botanical Garden Press, pp. 134–251.

Jiménez, L.C., Bogotá, R.G., Rangel, J.O., 2008. Atlas palinológico de la Amazonía Colombiana – las familias mas ricas en especies. In: Rangel, J.O. (Ed.), Colombia Diversidad Biótica VII: Vegetación, Palinología y Paleoecología de la Amazonía Colombiana. Instituto Ciencias Naturales Universidad Nacional de Colombia, pp. 217–416.

Latrubesse, E., Cozzuol, M., da Silva-Caminha, S., Rigsby, C., Absy, M., Jaramillo, C., 2010. The Late Miocene paleogeography of the Amazon Basin and the evolution of the Amazon River system. Earth-Sci. Rev. 99 (3–4):99–124. http://dx.doi.org/10.1016/j.earscirev.2010.02.005.

Lease, R.O., Ehlers, T.A., 2013. Incision into the Eastern Andean Plateau during Pliocene cooling. Science 341:774–776. http://dx.doi.org/10.1126/science.1239132.

Leier, A., McQuarrie, N., Garzione, C., Eiler, J., 2013. Stable isotope evidence for multiple pulses of rapid surface uplift in the Central Andes, Bolivia. Earth Planet. Sci. Lett. 371–372:49–58. http://dx.doi.org/10.1016/j.epsl.2013.04.025.

Leite, F.P.R., 2006. Palinologia da Formação Solimões, Neógeno da Bacia do Solimões, Estado do Amazonas: Implicações paleoambientais e bioestratigráficas. Ph.D. Thesis. Universidade de Brasília (138 pp).

Lorente, M.A., 1986. Palynology and palynofacies of the Upper Tertiary in Venezuela. Dissertationes Botanicae 99 (222 pp).

Marchant, R., Almeida, L., Behling, H., Berrio, J.C., Bush, M., Cleef, A., Duivenvoorden, J., Kappelle, M., De Oliveira, P., de Oliveira-Filho, A.T., Lozano-Garcia, S., Hooghiemstra, H., Ledru, M., Ludlow-Wiechers, B., Markgraf, V., Mancini, V., Paez, M., Prieto, A., Rangel, O., Salgado-Labouriau, M.L., 2002. Distribution and ecology of parent taxa of pollen lodged within the Latin American Pollen Database. Rev. Palaeobot. Palynol. 121:1–75. http://dx.doi.org/10.1016/S0034-6667(02)00082-9.

Martini, E., 1971. Standard Tertiary and Quaternary calcareous nannoplankton zonation. In: Farinacci, A. (Ed.), Proceedings II Planktonic Conference, Plankton Conference. 2, pp. 739–785. Roma.

Mayorga, E., Logsdon, M.G., Ballester, M.V.R., Richey, J.E., 2012. LBA-ECO CD-06 Amazon River Basin Land and Stream Drainage Direction Maps. Data set. http://dx.doi.org/10.3334/ORNLDAAC/1086 (Available on-line [http://daac.ornl.gov] from Oak Ridge National Laboratory Distributed Active Archive Center, Oak Ridge, Tennessee, U.S.A.).

McClain, M.E., Naiman, R.J., 2008. Andean influences on the biogeochemistry and ecology of the Amazon River. Bioscience 58 (4):325–338. http://dx.doi.org/10.1641/B580408.

McDaniel, D.K., McLennan, S.M., Hanson, G.N., 1997. Provenance of the Amazon Fan muds: constraints from Nd and Pb isotopes. In: Flood, R.D., Piper, D.J.W., Klaus, A., Peterson, L.C. (Eds.), Proceedings of the Ocean Drilling Program, Scientific Results. 155, pp. 169–176.

Meade, R.H., 1994. Suspended sediments of the modern Amazon and Orinoco rivers. Quat. Int. 21:29–39. http://dx.doi.org/10.1016/1040-6182(94)90019-1.

Mildenhall, D.C., Orpin, A.R., 2010. Terrestrial palynology from marine cores as an indicator of environmental change for the Waipaoa Sedimentary System and north-eastern New Zealand. Mar. Geol. 270:227–234. http://dx.doi.org/10.1016/j.margeo.2009.11.005.

Milliman, J.D., 1979. Morphology and structure of Amazon Upper Continental Margin. AAPG Bull. 63 (6), 934–950.

Milliman, J.D., 2001. River inputs. In: Steele, J.H., Turekian, K.K., Thorpe, S.A. (Eds.), Encyclopedia of Ocean Sciences. 4:pp. 2419–2427. http://dx.doi.org/10.1006/rwos.2001.0074.

Molnar, P., 2004. Late Cenozoic increase in accumulation rates of terrestrial sediment: how might climate change have affected erosion rates? Annu. Rev. Earth Planet. Sci. 32:67–89. http://dx.doi.org/10.1146/annurev.earth.32.091003.143456.

Molnar, P., England, P., 1990. Late cenozoic uplift of mountain ranges and global climate change: chicken or egg? Nature 346:29–34. http://dx.doi.org/10.1038/346029a0.

Montes, C., Cardona, A., Jaramillo, C., Pardo, A., Silva, J.C., Valencia, V., Ayala, C., Pérez-Angel, L.C., Rodriguez-Parra, L.A., Ramirez, V., Niño, H., 2015. Middle Miocene closure of the Central American Seaway. Science 248 (6231):226–229. http://dx.doi.org/10.1126/science.aaa2815.

Mora, A., 2007. Inversion Tectonics and Exhumation Processes in the Eastern Cordillera of Colombia. Ph.D. Thesis. Universität Potsdam, Potsdam (233 pp).

Mora, A., Baby, P., Roddaz, M., Parra, M., Brusset, S., Hermoza, W., Espurt, N., 2010. Tectonic history of the Andes and sub-Andean zones: implications for the development of the Amazon drainage basin. In: Hoorn, C., Wesselingh, F.P. (Eds.), Amazonia, Landscape and Species Evolution, a Look into the Past. Wiley-Blackwell, pp. 38–60.

Moscol-Olivera, M., Duivenvoorden, J.F., Hooghiemstra, H., 2009. Pollen rain and pollen representation across a forest-páramo ecotone in northern Ecuador. Rev. Palaeobot. Palynol. 157:285–300. http://dx.doi.org/10.1016/j.revpalbo.2009.05.008.

Moura, R.L., Amado-Filho, G.M., Moraes, F.C., et al., 2016. An Extensive Reef System at the Amazon River Mouth Science Advances. 2, e1501252. http://dx.doi.org/10.1126/sciadv.1501252 (39 authors).

Mulch, A., Uba, C.E., Strecker, M.R., Schoenberg, R., Chamberlain, C.P., 2010. Late Miocene climate variability and surface elevation in the central Andes. Earth Planet. Sci. Lett. 290 (1):173–182. http://dx.doi.org/10.1016/j.epsl.2009.12.019.

Muller-Karger, F.E., McClain, C.R., Richardson, P.L., 1988. The dispersal of the Amazon's water. Nature 333:56–59. http://dx.doi.org/10.1038/333056a0.

Niemann, H., Haberzettl, T., Behling, H., 2009. Holocene climate variability and vegetation dynamics inferred from the (11,700 cal yr BP) Laguna Rabadilla de Vaca sediment record in the southeastern Ecuadorian Andes. The Holocene 19:307–316. http://dx.doi.org/10.1177/0959683608100575.

Nittrouer, C.A., DeMaster, D.J., 1986. Sedimentary processes on the Amazon continental shelf: past, present and future research. Cont. Shelf Res. 6 (1/2), 5–30.

Please cite this article as: Hoorn, C., et al., The Amazon at sea: Onset and stages of the Amazon River from a marine record, with special reference to Neogene plant turnover in ..., Glob. Planet. Change (2017), http://dx.doi.org/10.1016/j.gloplacha.2017.02.005

Nittrouer, C.A., DeMaster, D.J., 1996. The Amazon shelf setting: tropical, energetic, and influenced by a large river. Cont. Shelf Res. 16 (5/6), 553–573.

Nittrouer, C.A., Kuehl, S.A., DeMaster, D.J., Kowsmann, R.O., 1986. The deltaic nature of Amazon shelf sedimentation. Geol. Soc. Am. Bull. 97:444–458. http://dx.doi.org/10.1130/0016-7606(1986)97<444:TDNOAS>2.0.CO;2.

Nogueira, A.C.R., Silveira, R., Guimarães, J.T.F., 2013. Neogene–Quaternary sedimentary and paleovegetation history of the eastern Solimões Basin, central Amazon region. J. S. Am. Earth Sci. 46, 89–99.

Ochoa, D., Hoorn, C., Jaramillo, C., Bayona, G., Parra, M., De la Parra, F., 2012. The final phase of tropical lowland conditions in the axial zone of the Eastern Cordillera of Colombia: evidence from three palynological records. J. S. Am. Earth Sci. 39, 157–169.

O'Dea, A., Lessios, H.A., Coates, A.G., et al., 2016. Formation of the Isthmus of Panama. Sci. Adv. 2 (8), e1600883. http://dx.doi.org/10.1126/sciadv.1600883 (35 authors).

Olson, D.M., Dinerstein, E., Wikramanayake, E.D., Burgess, N.D., Powell, G.V.N., Underwood, E.C., D'Amico, J.A., Itoua, I., Strand, H.E., Morrison, J.C., Loucks, C.J., Allnutt, T.F., Ricketts, T.H., Kura, Y., Lamoreux, J.F., Wettengel, W.W., Hedao, P., Kassem, K.R., 2001. Terrestrial ecoregions of the world: a new map of life on Earth. Bioscience 51 (11):933–938. http://dx.doi.org/10.1641/0006-3568(2001)051[0933:TEOTWA]2.0.C.

Paillard, D., Labeyrie, L., Yiou, P., 1996. Macintosh program performs time-series analysis. EOS Trans. Am. Geophys. Union 77 (39):379. http://dx.doi.org/10.1029/96EO00259.

Parra, M., Mora, A., Jaramillo, C., Strecker, M.R., Sobel, E.R., Quiroz, L., Rueda, M., Torres, V., 2009. Orogenic wedge advance in the northern Andes: evidence from the Oligocene-Miocene sedimentary record of the Medina Basin, Eastern Cordillera, Colombia. GSA Bull. 121 (5/6):780–800. http://dx.doi.org/10.1130/B26257.1.

Pasley, M.A., Shepherd, D.B., Pocknall, D.T., Boyd, K.P., Andrade, V., Figueiredo, J.J.P., 2005. Sequence Stratigraphy and Basin Evolution of the Foz do Amazonas Basin, Brazil. Search and Discovery Article 10082. http://www.searchanddiscovery.com/documents/2005/pasley/index.htm (February 2017).

Peters, J.L., Murray, R.W., Sparks, J.W., Coleman, D.S., 2000. Terrigenous matter and dispersed ash in sediment from the Caribbean Sea: results from Leg 165. In: Leckie, R.M., Sigurdsson, H., Acton, G.D., Draper, G. (Eds.), Proceedings of the Ocean Drilling Program, Scientific Results. 165, pp. 115–124.

Piedade, M.T.F., Junk, W., D'Ângelo, S.A., Wittmann, F., Schöngart, J., Barbosa, K.M.N., Lopes, A., 2010. Aquatic herbaceous plants of the Amazon floodplains: state of the art and research needed. Acta Limnol. Bras. 22 (2), 165–178.

Poulsen, C.J., Ehlers, T.A., Insel, N., 2010. Onset of convective rainfall during gradual late Miocene rise of the Central Andes. Science 328:490–493. http://dx.doi.org/10.1126/science.1185078.

Raczek, I., Jochum, K.P., Hofmann, A.W., 2003. Neodymium and strontium isotope data for USGS reference materials BCR-1, BCR-2, BHVO-1, BHVO-2, AGV-1, AGV-2, GSP-1, GSP-2 and eight MPI-DING reference glasses. Geostand. Newslett. 27 (2), 173–179.

Regali, M., Uesugui, N., Santos, A., 1974. Palinologia dos sedimentos Meso-Cenozoicos do Brasil. Boletim Tecnico da Petrobras 17, 177–191.

Ribas, C.C., Aleixo, A., Nogueira, A.C.R., Miyaki, C.Y., Cracraft, J., 2012. A palaeobiogeographic model for biotic diversification within Amazonia over the past three million years. Proc. R. Soc. B 279:681–689. http://dx.doi.org/10.1098/rspb.2011.1120.

Roddaz, M., Hermoza, W., Mora, A., Baby, P., Parra, M., Christophoul, F., Brusset, S., Espurt, N., 2010. Cenozoic sedimentary evolution of the Amazonian foreland basin system. In: Hoorn, C., Wesselingh, F.P. (Eds.), Amazonia, Landscape and Species Evolution, a Look into the Past. Wiley-Blackwell, pp. 61–88.

Rossetti, D.F., de Toledo, P.M., Góes, A.M., 2005. New geological framework for Western Amazonia (Brazil) and implications for biogeography and evolution. Quat. Res. 63 (1):78–89. http://dx.doi.org/10.1016/j.yqres.2004.10.001.

Rossetti, D.F., Cohen, M.C.L., Tatumi, S.H., Sawakuchi, A.O., Cremon, É.H., Mittani, J.C.R., Bertani, T.C., Munita, C.J.A.S., Tudela, D.R.G., Yee, M., Moya, G., 2015. Mid-Late Pleistocene OSL chronology in western Amazonia and implications for the transcontinental Amazon pathway. Sediment. Geol. 330, 1–15.

Roubik, D.W., Moreno, J.E., 1991. Pollen and spores of Barro Colorado Island. Monographs in Systematic Botany 36. Missouri Botanical Garden Press, St. Louis (268 pp).

Salamanca, S., van Soelen, E.E., Teunissen-van Manen, M.L., Flantua, S.G.A., Santos, R.V., Roddaz, M., Dantas, E.L., van Loon, E., Sinninghe-Damste, J.S., Kim, J.-H., Hoorn, C., 2016. Amazon forest dynamics under changing abiotic conditions in the early Miocene (Colombian Amazonia). J. Biogeogr. http://dx.doi.org/10.1111/jbi.12769 (In press).

Seyler, F., Muller, F., Cochonneau, G., Guimaraes, L., Guyot, J.L., 2009. Watershed delineation for the Amazon sub-basin system using GTOPO30 DEM and a drainage network extracted from JERS SAR images. Hydrol. Process. 23 (22), 3173–3185.

Shephard, G.E., Müller, R.D., Liu, L., Gurnis, M., 2010. Miocene drainage reversal of the Amazon River driven by plate–mantle interaction. Nat. Geosci. 3:870–875. http://dx.doi.org/10.1038/NGEO1017.

Silva-Caminha, S.A.F., Jaramillo, C., Absy, M.L., 2010. Neogene palynology of the Solimões Basin. Palaeontogr. Abt. B 283, 1–67.

Simon, M.F., Grether, R., de Queiroz, L.P., Skemae, C., Pennington, R.T., Hughes, C.E., 2009. Recent assembly of the Cerrado, a neotropical plant diversity hotspot, by in situ evolution of adaptations to fire. Proc. Natl. Acad. Sci. U. S. A. 106 (48):20359–20364. http://dx.doi.org/10.1073/pnas.0903410106.

Simon, M.F., Pennington, T., 2012. Evidence for adaptation to fire regimes in the tropical savannas of the Brazilian Cerrado. Int. J. Plant Sci. 173 (6), 711–723.

Soares, E.F., Zálan, P.V., Figueiredo, J.J.P., Trosdtorf Jr., I., 2007. Bacia do Pará-Maranhão. Boletim de Geociências da Petrobrás 15 (2), 321–329.

Strömberg, C.A.E., 2011. Evolution of grasses and grassland ecosystems. Annu. Rev. Earth Planet. Sci. 39, 517–544.

Subramaniam, P., Yager, P.L., Carpenter, E.J., Mahaffey, C., Björkman, K., Cooley, S., Kustka, A.B., Montoya, J.P., Sañudo-Wilhelmy, S.A., Shipe, R., Capone, D.G., 2008. Amazon River enhances diazotrophy and carbon sequestration in the tropical North Atlantic Ocean. Proc. Natl. Acad. Sci. U. S. A. 105 (30):10460–10465. http://dx.doi.org/10.1073/pnas.0710279105.

Torres, V., Hooghiemstra, H., Lourens, L., Tzedakis, P.C., 2013. Astronomical tuning of long pollen records reveals the dynamic history of montane biomes and lake levels in the tropical high Andes during the Quaternary. Quat. Sci. Rev. 63:59–72. http://dx.doi.org/10.1016/j.quascirev.2012.11.004.

UNESCO, 1981. Vegetation Map of South America: Explanatory Notes. United Nations Educational, Scientific and Cultural Organisation, Paris.

Van 't Veer, R., Hooghiemstra, H. (Eds.), 2000. Montane forest evolution during the last 650,000 yr in Colombia: a multivariate approach based on pollen record Funza-IJ. Quat. Sci. 15, 329–346.

Varol Research, 2004. Nannofossil Biostratigraphy of BP Offshore Well. Internal Report. Agência Nacional do Petróleo, Gás Natural e Biocombustíveis, Brazil.

Wanderley-Filho, J.R., Eiras, J.F., da Cruz, P.R., Cunha, van der Ven, 2010. The Paleozoic Solimões and Amazonas basins and the Acre foreland basin of Brazil. In: Hoorn, C., Wesselingh, F.P. (Eds.), Amazonia, Landscape and Species Evolution, a Look Into the Past. Wiley-Blackwell, pp. 29–37.

Watts, A.B., Rodger, M., Peirce, C., Greenroyd, C.J., Hobbs, R.W., 2009. Seismic structure, gravity anomalies, and flexure of the Amazon continental margin, NE Brazil. J. Geophys. Res. 114, B07103. http://dx.doi.org/10.1029/2008JB006259.

Weng, C.Y., Bush, M.B., Silman, M.R., 2004. An analysis of modern pollen rain on an elevational gradient in southern Peru. J. Trop. Ecol. 20:113–124. http://dx.doi.org/10.1017/S0266467403001068.

Wesselingh, F.P., 2006. Molluscs from the Miocene Pebas Formation of Peruvian and Colombian Amazonia. Scr. Geol. 133, 19–290.

Wilkinson, M.J., Marshall, L.G., Lundberg, J.G., Kreslavsky, M.H., 2010. Megafan Environments in Northern South America and their impact on Amazon Neogene aquatic ecosystems. In: Hoorn, C., Wesselingh, F. (Eds.), Amazonia, Landscape and Species Evolution, a Look into the Past. Wiley-Blackwell:pp. 162–184. http://dx.doi.org/10.1002/9781444306408.ch10.

Wilson, K.E., Maslin, M.A., Burns, S.J., 2011. Evidence for a prolonged retroflection of the North Brazil current during glacial stages. Palaeogeogr. Palaeoclimatol. Palaeoecol. 301:86–96. http://dx.doi.org/10.1016/j.palaeo.2011.01.003.

Yoon, J.-H., Zeng, N., 2010. An Atlantic influence on Amazon rainfall. Clim. Dyn. 34 (2), 249–264.

Please cite this article as: Hoorn, C., et al., The Amazon at sea: Onset and stages of the Amazon River from a marine record, with special reference to Neogene plant turnover in ..., Glob. Planet. Change (2017), http://dx.doi.org/10.1016/j.gloplacha.2017.02.005